THE UNIVERSITY OF MICHIGAN

INDUSTRY PROGRAM OF THE COLLEGE OF ENGINEERING

MOTION OF A SPHERE IN A ROTATING FLUID
AT SMALL REYNOLDS NUMBERS

Philip Davis

Doctoral Committee:

>   Professor Chia-Shun Yih, Chairman
>   Professor Samuel K. Clark
>   Associate Professor William P. Graebel
>   Professor Arnold M. Kuethe
>   Professor Victor L. Streeter

ACKNOWLEDGMENTS

TABLE OF CONTENTS

LIST OF FIGURES

LIST OF FIGURES (CONT'D)

I. INTRODUCTION

The motion of solid bodies in rotating, inviscid and imcompressible fluids was studied by Taylor, [8,9,10,11,12,13] Proudman [14] and Grace, [2,3,4,5] who published several papers during the period 1915-26. Since then many other researchers have made contributions to this field. In contrast, comparatively little work in this field has taken the effects of viscosity into account. It seems desirable, therefore, to investigate the motion of solid bodies in a rotating viscous fluid. A logical beginning to such an investigation is a study of the motion of a symmetrical body, such as a sphere, at low Reynolds numbers. Proudman [14] and Taylor [8,10,11] predicted by theory and later Taylor [12] confirmed by experiment that the slow motion of a sphere along the axis of a rotating inviscid fluid is two dimensional. That is, the velocity components are independent of the coordinate z measured along the axis of rotation. Just what effect does viscosity have on this motion? From a different point of view, what effect will rotation have on the terminal velocity of a sphere in the Stokes range? These questions have motivated this study.

The present work explores two types of motion of a sphere encountered in a rotating viscous liquid when the Reynolds number, based on the translational velocity parallel to the axis of rotation, is less than unity. These are (1) the slow steady rise of a sphere along the axis of a uniformly rotating viscous fluid, and (2) the spiraling motion of a sphere of greater density than that of the fluid, away from the axis of a uniformly rotating viscous fluid.

It has been found that viscosity acts to destroy the two-dimensionality predicted by Taylor and Proudman for weak steady motion of an inviscid fluid under rotation, and that the effect of rotation is to reduce the speed of fall or rise of the sphere in the Stokes range. Specific results are presented in Chapter V. It is hoped that the systematic experimental results obtained will provide an initial step toward solving certain problems encountered in industry, such as the separation of solid foreign materials from a viscous liquid by means of rotation, or the separation of wood fibers in a viscous suspension from dirt particles by the same means.

II. THE GOVERNING EQUATIONS FOR MOTION ALONG THE AXIS

A. The Differential System

The problem considered here is the motion of a sphere along the axis of an infinitely long cylinder which is filled with a viscous liquid and rotating about its axis. It is convenient to use a cartesian reference frame which rotates at the same angular speed ω as the cylinder and which has its origin at the center of the sphere. The coordinates with respect to this frame are denoted by x, y, z, with the z-axis coinciding with the axis of the cylinder. The coordinates with respect to the inertial frame of reference with origin at the center of the sphere are denoted by X, Y, and Z, as shown in Figure 1.
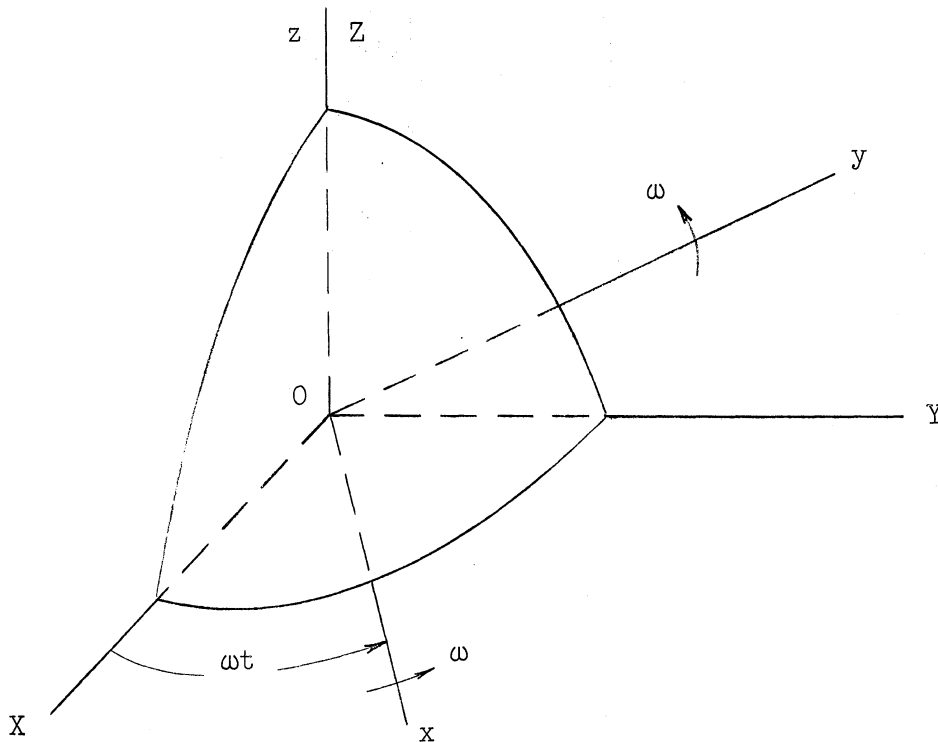
Figure 1. Reference Frames

The components of the velocity of the fluid relative to the rotating frame are denoted by u, v, and w. At a time that the coordinates x, y, and z momentarily coincide with X, Y, and Z, the velocity components in the inertial frame of reference are

$$U = u - \omega y, \tag{1}$$

$$V = v + \omega x, \tag{2}$$

and

$$W = w. \tag{3}$$

For a flow which is independent of time, the choice of the origin of time at which the rotating axis coincide with the inertial axis is immaterial.

The differential system for the fluid medium to be satisfied between the boundaries are the Navier-Stokes equations along with the continuity equation. Substitution of (1), (2), and (3) into these equations gives[6]

$$\frac{Du}{Dt} - 2\omega v - \omega^2 x = - \frac{1}{\rho} \frac{\partial p}{\partial x} + F_x + \nu \nabla^2 u, \tag{4}$$

$$\frac{Dv}{Dt} + 2\omega u - \omega^2 y = - \frac{1}{\rho} \frac{\partial p}{\partial y} + F_y + \nu \nabla^2 v, \tag{5}$$

$$\frac{Dw}{Dt} = - \frac{1}{\rho} \frac{\partial p}{\partial z} + F_z + \nu \nabla^2 w, \tag{6}$$

$$\frac{\partial u}{\partial x} + \frac{\partial v}{\partial y} + \frac{\partial w}{\partial z} = 0, \tag{7}$$

where

$$\frac{D}{Dt} = \frac{\partial}{\partial t} + u \frac{\partial}{\partial x} + v \frac{\partial}{\partial y} + w \frac{\partial}{\partial z} \, ,$$

$$\nabla^2 = \frac{\partial^2}{\partial x^2} + \frac{\partial^2}{\partial y^2} + \frac{\partial^2}{\partial z^2} \, ,$$

F_x, F_y, and F_z are the body forces per unit mass in the

x, y, and z directions respectively,

v = kinematic viscosity of the fluid,

and

ρ = mass density of the fluid.

$\frac{\partial}{\partial t}$ now represents the change with respect to time relative to the

rotating reference frame when x, y, and z are constant.

The size and density of the sphere and the viscosity and den-

sity of the liquid may all be chosen such that the translational velocity

(W_ω) of the sphere along the z-axis will be small. It is assumed here

that the Reynolds number based on W_ω and the sphere diameter, d, is

less than unity. Hence u, v, and w are small compared with v/d for

all values of ω. Further, we consider here only the motion after terminal

velocity of the sphere has been reached. The experiments show that the

sphere reaches a terminal velocity rapidly. The unsteady flow problem may

now be looked upon as a steady-flow problem by considering the center of

the sphere as fixed, with a uniform velocity equal and opposite to W_ω

superposed on the rotating liquid and cylinder. With these assumptions,

one can neglect the substantial derivatives of the velocity components in Equations (4), (5), and (6). The only body force present in this treatment is that due to gravity. Therefore, if

$$p_d = p - p_s ,$$

in which p_s is the hydrostatic part of the pressure and if

$$P \equiv \frac{p_d}{\rho} - \frac{\omega^2}{2} (x^2 + y^2), \tag{8}$$

the differential system (4) through (7) reduces to

$$-2\omega v = -\frac{\partial P}{\partial x} + \nu \nabla^2 u, \tag{9}$$

$$2\omega u = -\frac{\partial P}{\partial y} + \nu \nabla^2 v, \tag{10}$$

$$0 = -\frac{\partial P}{\partial z} + \nu \nabla^2 w, \tag{11}$$

and

$$\frac{\partial u}{\partial x} + \frac{\partial v}{\partial y} + \frac{\partial w}{\partial z} = 0. \tag{7}$$

This linear system of partial differential equations along with the appropriate boundary conditions constitute the boundary value problem which governs the flow of fluid between the boundaries of the sphere and the cylinder. Once u, v, w and P are determined, the pressure and shear drag on the sphere surface may be obtained by integration.

It is not always possible to decide whether the velocities associated with a particular type of flow will or will not be small;[7]

therefore, should the results of the problem formulated here not conform with the experimental results given in Chapter 5, the assumption of slow motion is invalid.

Cross differentiation and addition of (9), (10) and (11) along with the use of (7) gives

$$\nabla^2 P = 2\omega \left(\frac{\partial v}{\partial x} - \frac{\partial u}{\partial y} \right) = 2\omega \zeta , \tag{12}$$

where ζ represents the component of the vorticity vector in the z-direction. Cross differentiation and subtraction of (9) and (10) along with the use of (7) gives

$$\nu \nabla^2 \zeta = -2\omega \frac{\partial w}{\partial z} . \tag{13}$$

The combination of (11), (12) and (13) gives the following equation to be solved

$$\nu \nabla^2 \nabla^2 \nabla^2 w + 4\omega^2 \frac{\partial^2 w}{\partial z^2} = 0 . \tag{14}$$

B. Effect of the Coriolis Terms

It is worthwhile here to point out the similarities of the present problem for the special case of a cylinder with infinite radius to the classical problem solved by Stokes for the slow motion of a sphere in a non-rotating infinite fluid. However, this problem should not be labeled "Strokes flow in a rotating fluid" until the assumed slow motion is verified with the experimental results herein. If the Coriolis

acceleration components, $-2\omega v$ and $2\omega u$, are neglected in equations (9) and (10), the system reduces to a set of equations quite similar to those of Stokes with the only differences being that p in the Stokes problem is now replaced by P and the velocity components here are relative velocities whereas they represent absolute values in the Stokes problem. Integration of the resulting pressure and shear stresses over the surface of the sphere gives results identical to Stokes' for the pressure drag and shear drag. Thus it is the effect of the Coriolis acceleration that leads to a drag on the sphere greater than the Stokes drag.

C. Boundary Conditions

On the wall of the cylinder containing the fluid, the no-slip condition requires that

$$u = v = 0 \text{ and } w = W_\omega \text{ for } \sqrt{x^2 + y^2} = D/2 \text{ and all } z, \quad (15)$$

in which D is the diameter of the cylinder, and W_ω is the velocity superposed on the liquid and the cylinder and is equal in magnitude to the terminal velocity of the sphere.

The boundary conditions far away from the sphere are

$$u = v = 0, \ w = W_\omega \text{ and } p_d = 1/2 \ \omega^2 \rho (x^2 + y^2)$$

$$\text{for } z = \pm \infty \text{ and } \sqrt{x^2 + y^2} \le D/2 . \quad (16)$$

There still remains to specify the boundary conditions on the sphere surface. The angular rotation of the sphere is governed by Euler's equation of motion for a rigid body. Euler's equation shows that the angular acceleration of the sphere must be zero for the torque on the sphere to be zero. Thus, the sphere rotates at a constant angular velocity. It has been verified experimentally by the writer that for W_ω in the Stokes range ($W_\omega \leq 0.0352$ ft/sec for the experiments herein) the sphere rotates at the same angular velocity as the cylinder. This was accomplished by means of a Strobotac light. The light was first synchronized on two reference marks 180 degrees apart on the rotating cylinder then checked for synchronization on two reference marks 180 degrees apart on the sphere. This was done for angular speeds from 60 to 400 rpm. Thus, the boundary conditions at the sphere surface are

$$u = v = w = 0 \quad \text{for} \quad \sqrt{x^2 + y^2 + z^2} = d/2 = a , \quad (17)$$

where a and d are the sphere radius and diameter respectively. However, this is true only for very low values of W_ω, and at any rate one should not have to rely upon this experimental fact in the mathematical formulation of the problem. The speed of rotation of the sphere is determined by the condition that the torque on it should be zero.

III. DIMENSIONAL ANALYSIS

A. Motion Along the Axis

The dependent variable and the variable to be measured experimentally is the terminal velocity of the sphere along the axis of rotation, i.e., W_ω . The functional equation is

$$W_\omega = f(d, D, \omega, \gamma_\ell - \gamma_s, \mu, \rho_\ell) \, , \qquad (18)$$

where γ represents specific weight, μ the viscosity and the subscripts ℓ and s refer to liquid and sphere respectively. The other variables have the same meaning as in the previous chapter. The diameters of the sphere and cylinder represent the geometry, $\gamma_\ell - \gamma_s$ is proportional to the driving force on the sphere, μ represents the viscous force, ρ_ℓ is included because of the Coriolis acceleration of the fluid particles and ω is an independent variable which determines the magnitude of this acceleration.

Equation (18) can now be reduced by arranging the seven pertinent variables into four non-dimensional ratios (π - terms) according to the Buckingham π - theorem. There are several sets of π - terms in which the variables in Equation (18) may be arranged but it is desired here to have W_ω and ω appear in the first power in only one π - term each so that the data can be advantageously presented. Using d, $\gamma_\ell - \gamma_s$ and μ as repeating variables gives

$$\pi_1 = \frac{W_\omega}{d^2} \left(\frac{\mu}{\gamma_\ell - \gamma_s} \right), \quad \pi_2 = \frac{\omega}{d} \left(\frac{\mu}{\gamma_\ell - \gamma_s} \right), \quad \pi_3 = d/D \quad \text{and}$$

$$\pi_4 = \frac{(\gamma_\ell - \gamma_s)}{\rho_\ell} \frac{d^3}{v^2} \, , \qquad (19)$$

for the four π - terms. Equation (18) now reduces to

$$W_\omega = d^2 \frac{(\gamma_\ell - \gamma_s)}{\mu} f\left[d/D , \frac{\omega}{d} \left(\frac{\mu}{\gamma_\ell - \gamma_s}\right) , \left(\frac{\gamma_\ell - \gamma_s}{\rho_\ell}\right) \frac{d^3}{v^2} \right] , \qquad (20)$$

Equation (20) furnishes the guide for experimentation. For a particular sphere, cylinder and liquid, π_3 and π_4 are constant if the temperature is held constant, π_2 can be controlled by controlling the angular speed of the cylinder and π_1 can then be measured. The results can then be presented in two-dimensional plots as shown in Figure 2.

B. Motion Out From the Axis

The dependent variable chosen for this motion is the distance (L) measured along the axis of rotation that the sphere moves while at the same time moving a radial distance of D/2. The sphere is heavier than the liquid for this type of motion and the motion is initiated by releasing the sphere at the axis of rotation on the free surface. It is assumed that the path of motion of the sphere will lie on the surface of a cone whose axis is the axis of rotation and whose cone angle is β = 2 COT^{-1} 2 L/D . The angle between the cone and the horizontal is θ = TAN^{-1} 2 L/D . The scheme is shown in Figure 3.

The functional equation is

$$L = f(d, D, \gamma_s - \gamma_\ell , \omega, \mu, \rho_\ell , \rho_s) . \qquad (21)$$

The density of the sphere is included in this motion because the sphere also undergoes acceleration.
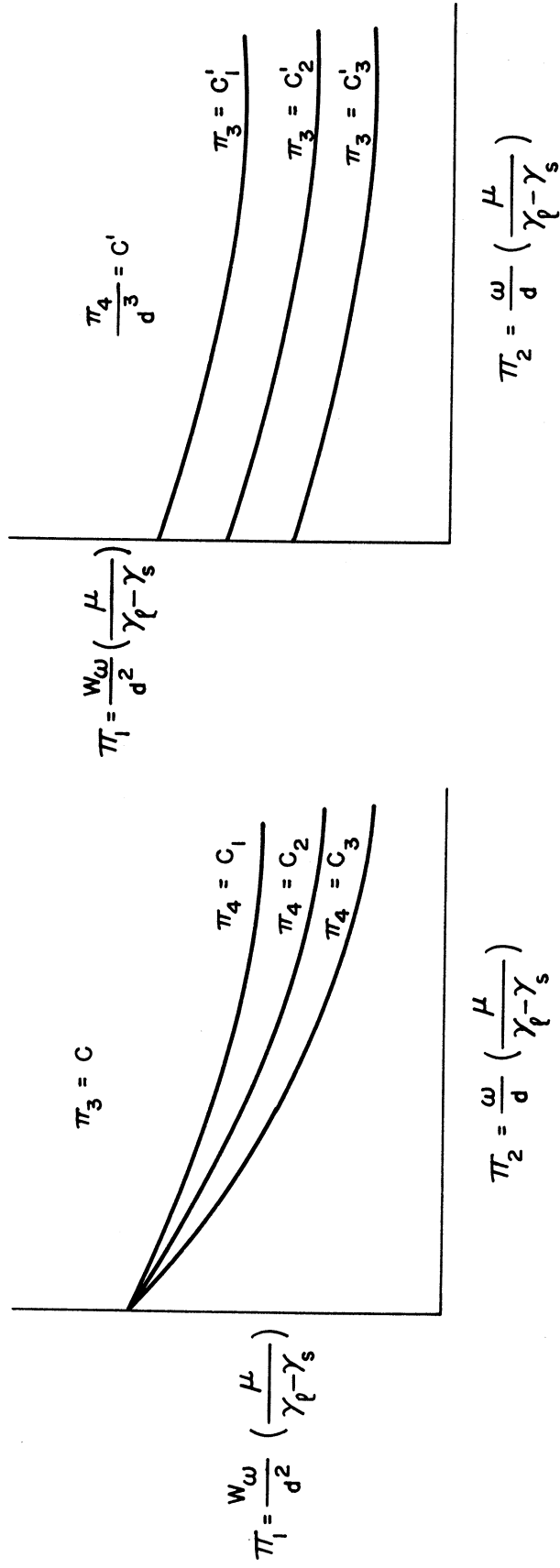
Figure 2. Sketch of the Relationship Between π_1, & π_2 for Motion Along the Axis.
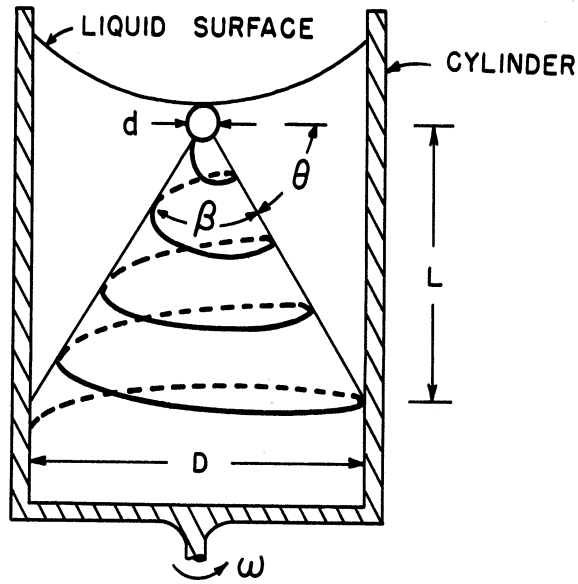
Figure 3. Definition Sketch for Motion out
From the Axis.

$$\pi_1^* = TAN\,\theta = \frac{2L}{D}$$

$$\frac{\pi_4^*}{d^3} = C^*$$

$$\pi_5^* = C_1^*$$

$$\pi_3^* = C_2^*$$

$$\pi_3^* = C_4^* \qquad \pi_3^* = C_3^*$$

$$\pi_2^* = \frac{\omega}{d}\left(\frac{\mu}{\gamma_s - \gamma_\ell}\right)$$

Figure 4. Sketch of the Relationship Between π_1^* & π_2^* for
Motion out From the Axis.

Here again the functional equation is reduced by means of the Buckingham π - theorem. Using d, $\gamma_s - \gamma_\ell$ and μ as repeating variables, the non-dimensional ratios become

$$\left[\frac{L}{d} \right], \left[\frac{\omega}{d} \left(\frac{\mu}{\gamma_s - \gamma_\ell} \right) \right], \left[\frac{d}{D} \right], \left[\frac{(\gamma_s - \gamm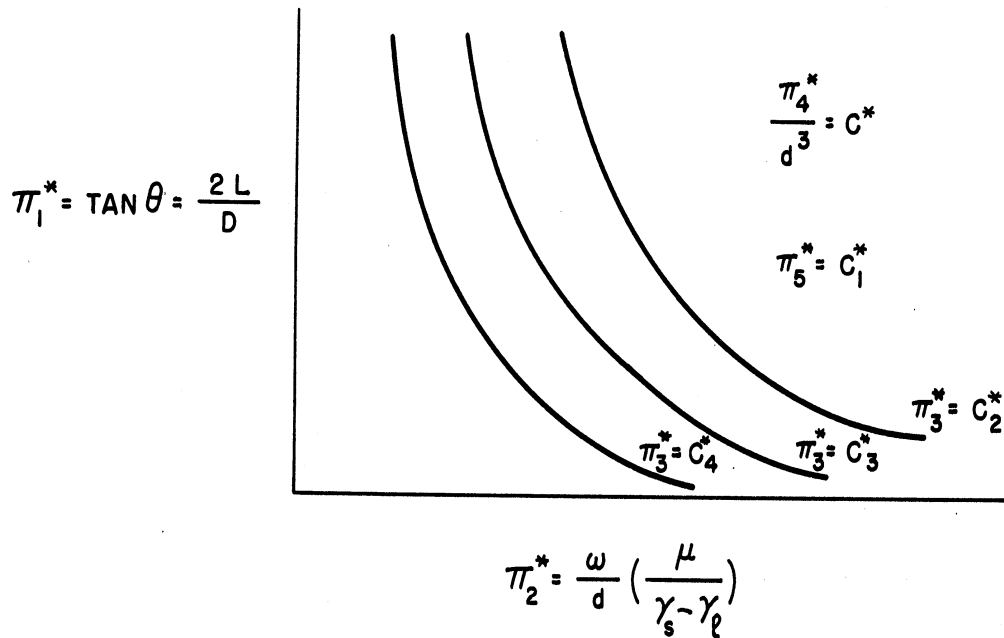a_\ell) \rho_\ell d^3}{\mu^2} \right] \text{ and } \left[\frac{(\gamma_s - \gamma_\ell) \rho_s d^3}{\mu^2} \right]. \quad (22)$$

For more meaningful ratios, L/d is changed to $2L/D$ ($D/2$ is also a pertinent length) and the ratio of the last two π - terms is used in place of the last one in (22), i.e., $\rho s/\rho \ell$. We now define

$$\pi_1^* = 2L/D, \quad \pi_2^* = \frac{\omega}{d} \left(\frac{\mu}{\gamma_s - \gamma_\ell} \right), \quad \pi_3^* = d/D, \quad \pi_4^* = \frac{(\gamma_s - \gamma_\ell)}{\rho \ell} \frac{d^3}{v^2}, \text{ and}$$

$$\pi_5^* = \frac{\rho s}{\rho \ell}, \quad (23)$$

which are the pertinent dimensionless parameters for experimental purposes. Equation (21) now reduces to

$$L = \frac{D}{2} f \left[\frac{\omega}{d} \left(\frac{\mu}{\gamma_s - \gamma_\ell} \right), \frac{d}{D}, \frac{(\gamma_s - \gamma_\ell)}{\rho \ell} \frac{d^3}{v^2}, \frac{\rho s}{\rho \ell} \right]. \quad (24)$$

Note that for a particular sphere, a particular cylinder and a particular liquid, π_3^*, π_4^* and π_5^* are constants if the temperature is held constant, π_2^* can be controlled by controlling the angular speed of the cylinder and π_1^* can be observed experimentally. The results can then be shown graphically as in Figure 4.

IV. EXPERIMENTAL EQUIPMENT AND PROCEDURE

A. Apparatus

The apparatus consists mainly of a clear plastic cylinder 30 inches long with a 5-inch inside diameter filled with castor oil and mounted on an adjustable-speed turn-table as shown in Figure 5. The turn-table is driven by a Servo-Tek adjustable speed drive. This drive consists mainly of a 3/4 horsepower series motor which is supplied a controlled current by means of a thyrotron rectifier and feedback arrangement. Changes in load of as much as 50% or a change in supply voltage of ± 10 volts results in a speed change of less than 1/2 of 1% of the rated speed of the motor.*

The speed of rotation is determined by use of an electronic counter, produced by the Hewlett Packard Company, and a magnetic transducer. The transducer is mounted close to a steel gear which turns with the cylinder. The gear teeth actuate the transducer which in turn supplies the electronic counter with an input signal.

B. Selection of Fluid and Spheres

Castor oil was found to be the most desirable for these experiments because its viscosity is high and its change of viscosity with temperature is relatively large in comparison with other common oils and liquids. The high change in viscosity with temperature made it easier to vary the viscosity. Also, its chemical and physical characteristics

---

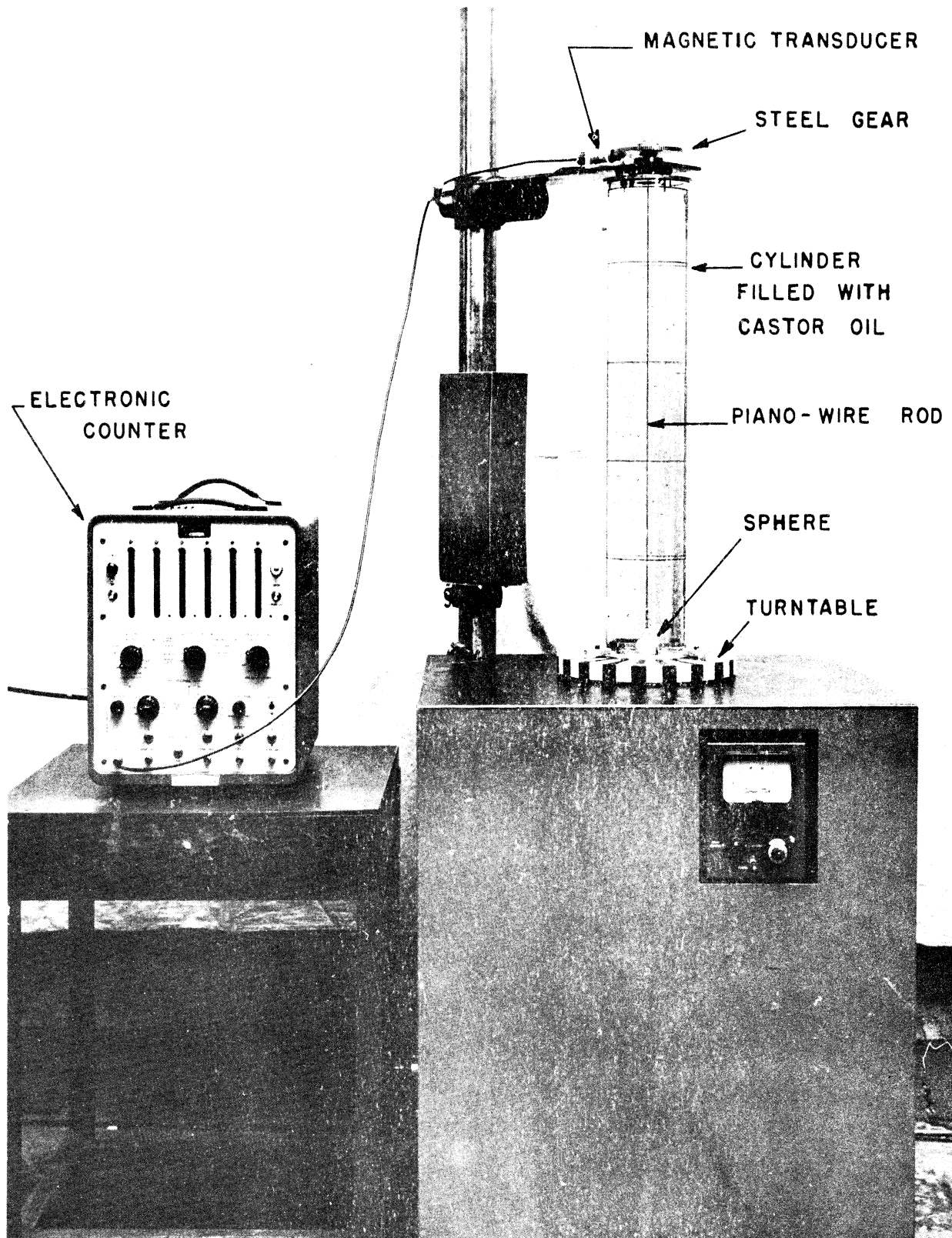* Servo-Tek Adjustable-Speed Drives, catalog 11058.

MAGNETIC TRANSDUCER

STEEL GEAR

CYLINDER
FILLED WITH
CASTOR OIL

PIANO-WIRE ROD

SPHERE

TURNTABLE

ELECTRONIC
COUNTER

Figure . Equipment Picture.

do not change appreciably with age if it is kept under normal indoor storage conditions. The variation of the physical properties with temperature for the U.S.P. grade castor oil used is shown in Appendix A, Figure 18.*

For observation of motion along the axis, it was necessary to use spheres which are slightly less dense than the castor oil so that they would remain on the axis and the motion along the axis would be small enough for the Reynolds number to be less than unity. Polyethylene spheres (S.G. = 0.91 to 0.925) were found satisfactory for this purpose.

For observation of motion out from the axis, it was necessary to use spheres slightly more dense than the castor oil. Nylon spheres (S.G. = 1.14) were found satisfactory for this experiment and yielded a Reynolds number based on the translational velocity parallel to the axis of rotation of less than unity.

C. Method For Observing Motion Along the Axis

Since the polyethylene spheres were less dense than the castor oil, they rose along the axis of rotation. The sphere was first pushed to the bottom center of the cylinder with a piano-wire rod. The cylinder of liquid was then set into rotation at the desired speed and a few seconds were allowed for the castor oil to attain solid body rotation. The piano-wire rod was then pulled out setting the sphere free to move

---

* This information was kindly supplied to the writer by the manufacturer, The Baker Castor Oil Company.

along the axis. By the time the sphere reached the test section, the
disturbance created by the piano-wire rod had decayed and the sphere
moved at essentially the terminal speed. The test section was one half
foot long and was located in the central portion of the cylinder in
order to minimize end effects. Since the motion was very slow, the
time for the sphere to travel one half foot along the axis was easily
measured with a stop-watch. Data could also be taken directly above
and below the main test section to verify that the sphere was not
accelerating.

Starting the cylinder from rest to the desired speed of
rotation created shear stresses in the liquid until it reached a solid
body rotation. Shear stresses were again created while bringing the
liquid back to rest after the data were taken for a particular value
of ω . These shear stresses created small amounts of heat which
affected the viscosity to some degree. Consequently, it was desirable
to measure the viscosity between each data point taken. This was done
when the liquid was quiescent by checking the rise velocity W_O of
the same sphere being used for the experiment and by using the well
known Stokes relation for an infinite fluid

$$\mu = \frac{d^2 (\gamma_\ell - \gamma_s)}{18 \, W_O} \tag{25}$$

along with the Francis equation[1] for wall effect correction

$$\frac{W_O}{W_\infty} = \left\{ \frac{1 - d/D}{1 - 0.475 \, d/D} \right\}^4 , \quad (d/D < 0.9) . \tag{26}$$

The non-dimensional ratios involving viscosity are then

$$\pi_1 = \frac{W\omega}{18\,W_0} \left\{ \frac{1 - d/D}{1 - 0.475\ d/D} \right\}^4 , \tag{27}$$

$$\pi_2 = \frac{\omega d}{18\,W_0} \left\{ \frac{1 - d/D}{1 - 0.475\ d/D} \right\}^4 , \tag{28}$$

and

$$\pi_4 = \frac{(18\,W_0)^2}{dg\ \left(1 - \frac{\gamma s}{\gamma \ell}\right)} \left\{ \frac{1 - 0.475\ d/D}{1 - d/D} \right\}^8 . \tag{29}$$

D. Method for Observing Motion Out from the Axis

The motion of the nylon spheres was composed of a downward, radial and rotational component since the density of the spheres used for this experiment was greater than that of the liquid. A sphere was released on the axis of rotation at the free surface after the cylinder of liquid was in solid-body rotation at the desired speed. A mark was placed on the cylinder wall where the sphere was released and also where it first touched the cylinder. The distance between these marks was the distance L shown in Figure 3. A scale was also placed along the bottom of the cylinder for the purpose of measuring radial distances less than D/2 since for small rotations the sphere traversed the entire length of the cylinder before it traveled a radial distance of D/2. The length L could then be determined by extrapolation.

V. RESULTS

A. Motion Along the Axis

Figures 6 through 13 represent the data in the form suggested in Figure 2(a), for eight spheres ranging in size from 1/4 inch to 1-1/8 inch in diameter. Figures 6(a) through 13(a) show the corresponding data in Figures 6 through 13 plotted to a log-log scale. The range of π_2 for each sphere is from 0 to 4. The data for each sphere are shown in a plot of π_1 versus π_2 for three constant values of π_4. π_4 was varied by varying the temperature of the castor oil.

Figure 14 represents the data in the form suggested in Figure 2(b), for eight values of π_3 when π_4/d^3 was held approximately constant. The relations given in the Appendix (page 50) for γ_ℓ and ρ_ℓ, with a quadratic approximation for the data given for μ in the Appendix (Figure 18), give

$$\frac{\pi_4}{d^3} = \frac{(3.739 - 2.289 \times 10^2 \text{ T})(1.911 - 7.113 \times 10^{-4} \text{ T})}{(160.494 \times 10^{-5} \text{ T}^2 - 308.609 \times 10^{-5} \text{ T} + 15{,}602.183 \times 10^{-5})^2} ,$$

$$(68°F \leq T \leq 86°F), \tag{30}$$

where T represents the temperature in degrees Fahrenheit. Equation (30) shows that π_4/d^3 is a function of temperature only. The oil temperature, which depended upon the ambient temperature of the laboratory at the time of a test, varied from a minimum of 70.25°F for $\pi_3 = 0.125$ to a maximum of 71.5°F for the values of π_3 of 0.225, 0.200 and 0.100, with the average temperature for the eight values of π_3 being 71.3°F. Hence
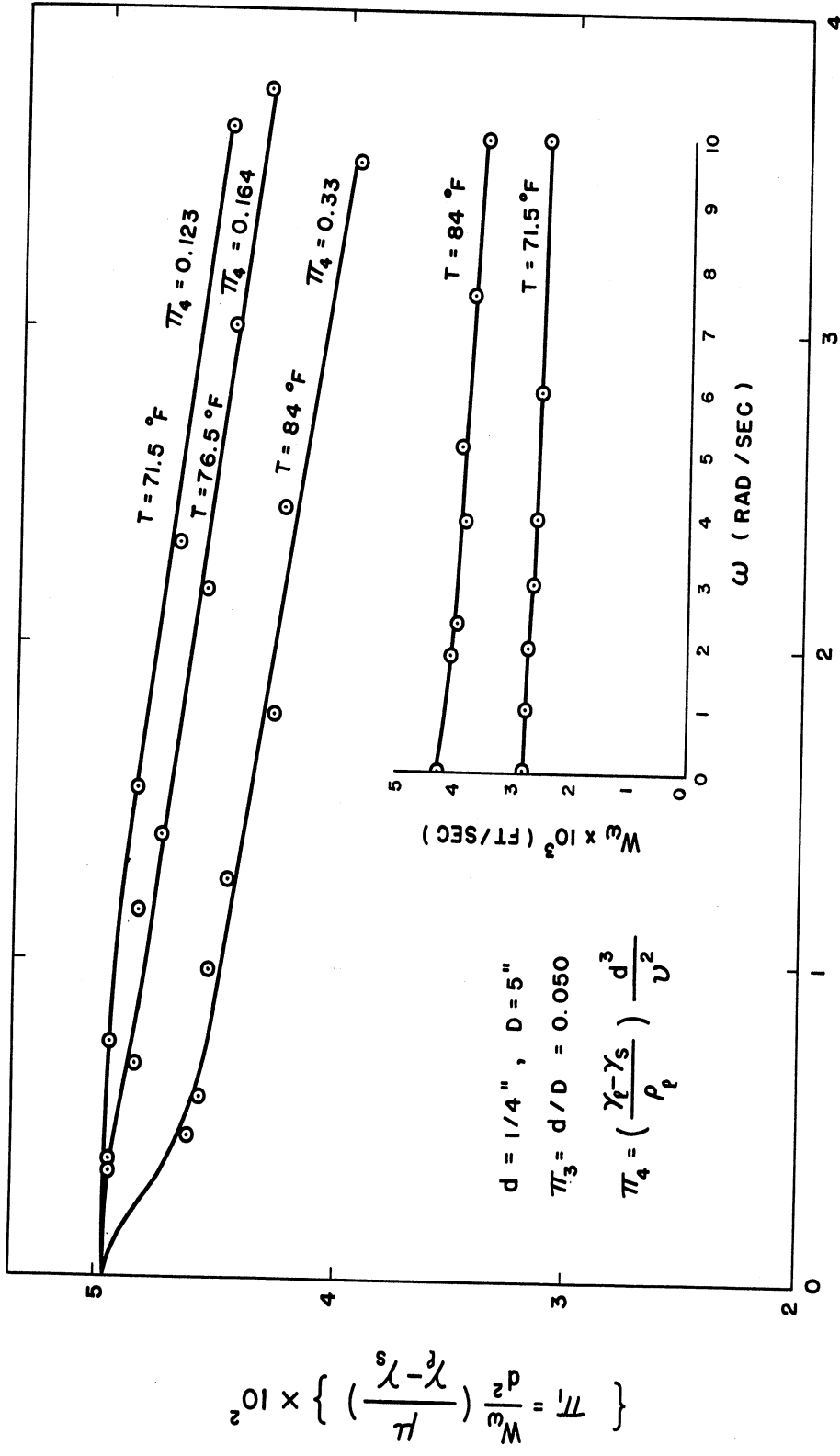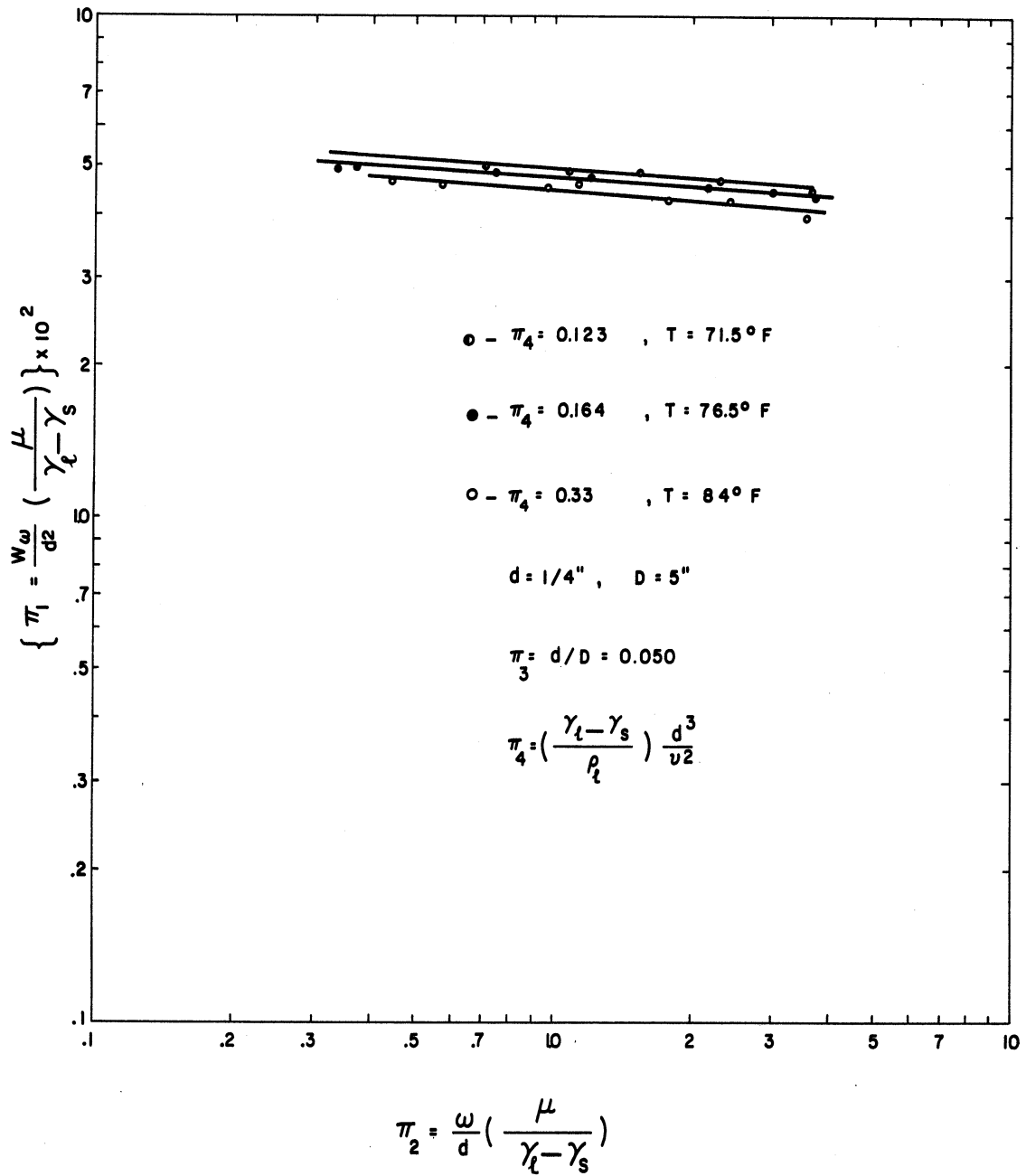
Figure 6. Curves of Constant π_4 for $\pi_3 = 0.050$.

$$\pi_2 = \frac{\omega}{d}\left(\frac{\mu}{\gamma_\ell - \gamma_s}\right)$$

Figure 6(a). Curves of Constant π_4 for $\pi_3 = 0.050$.
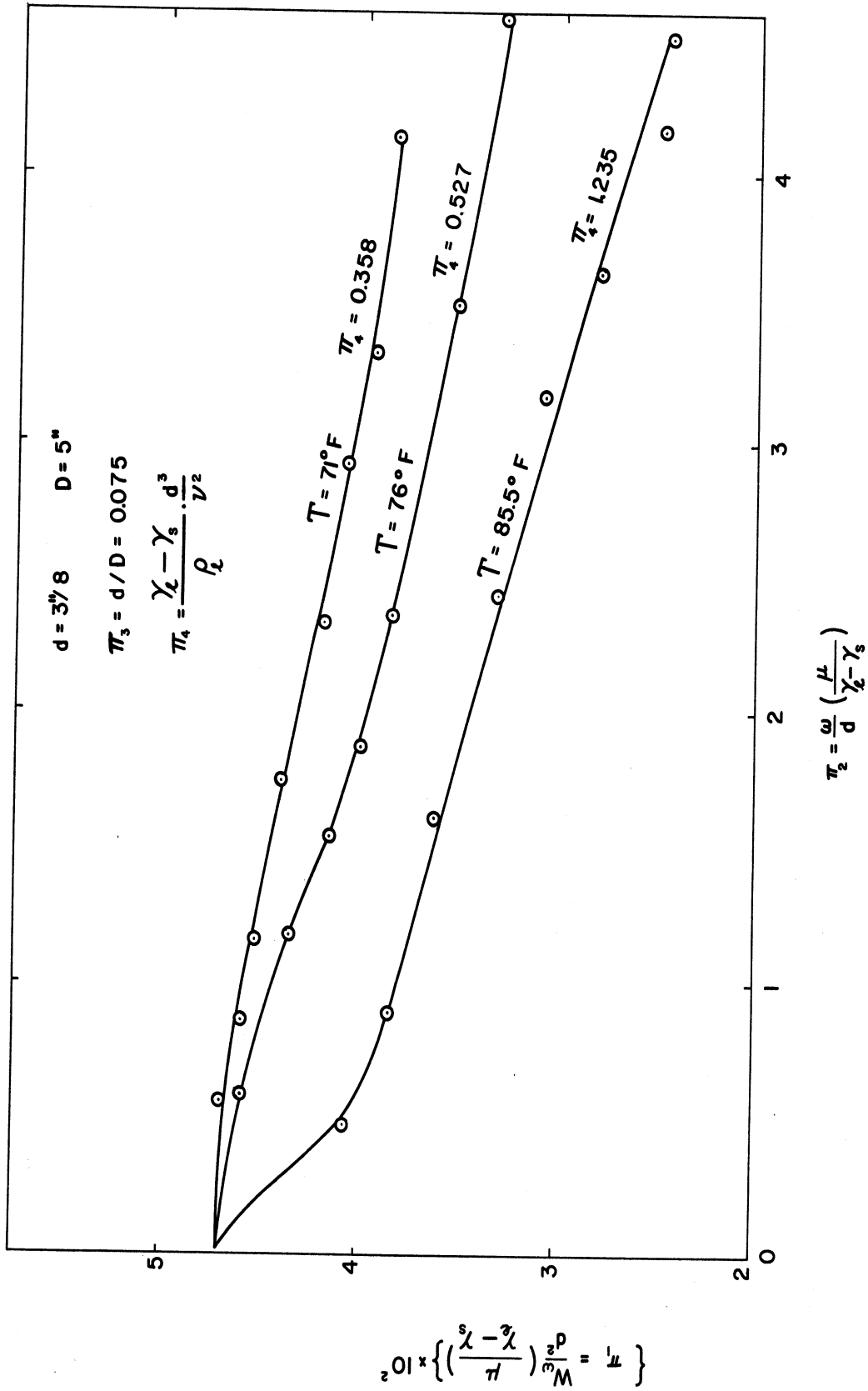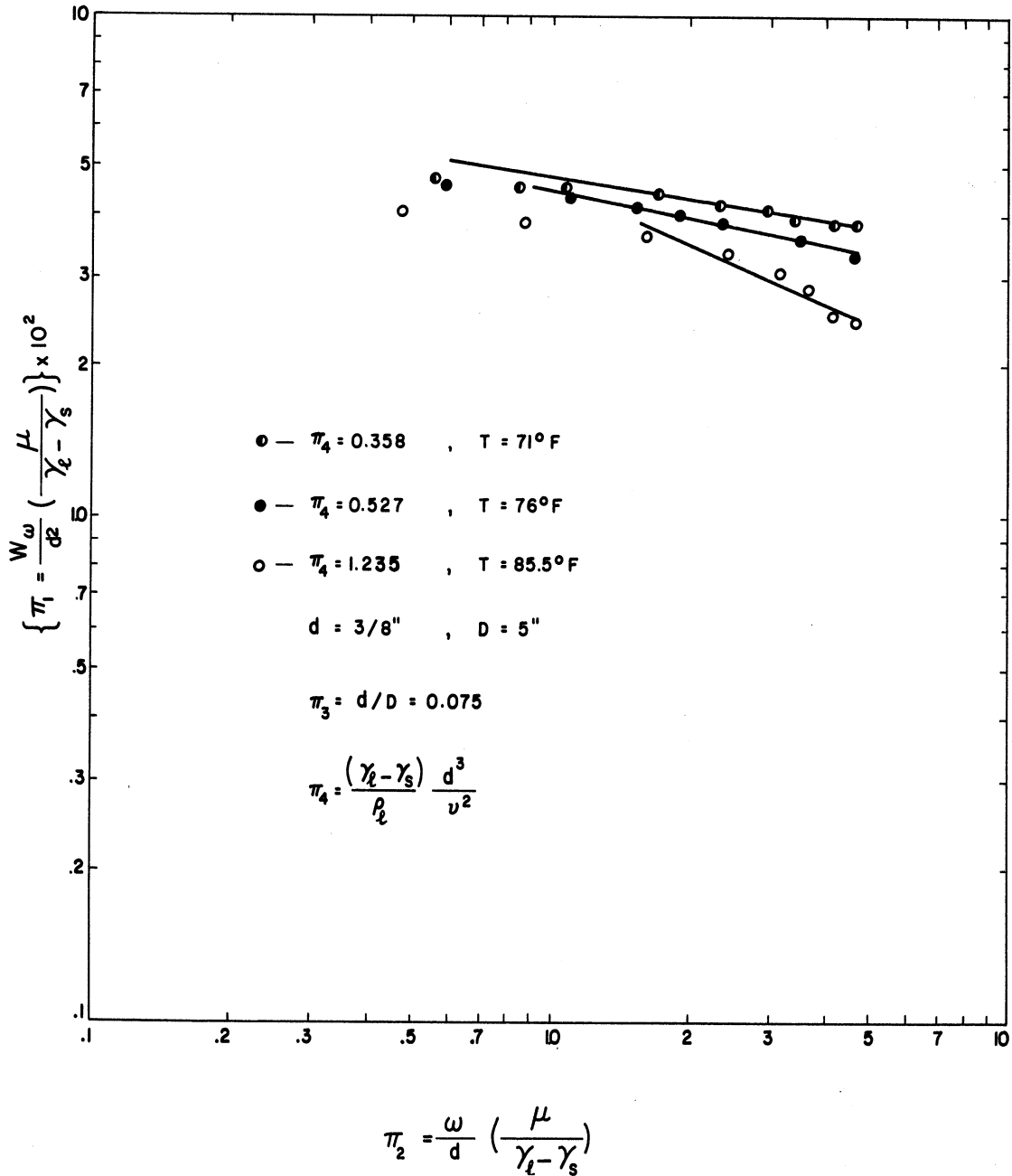
Figure 7. Curves of Constant π_4 for $\pi_3 = 0.075$.

Figure 7(a). Curves of Constant π_4 for $\pi_3 = 0.075$.
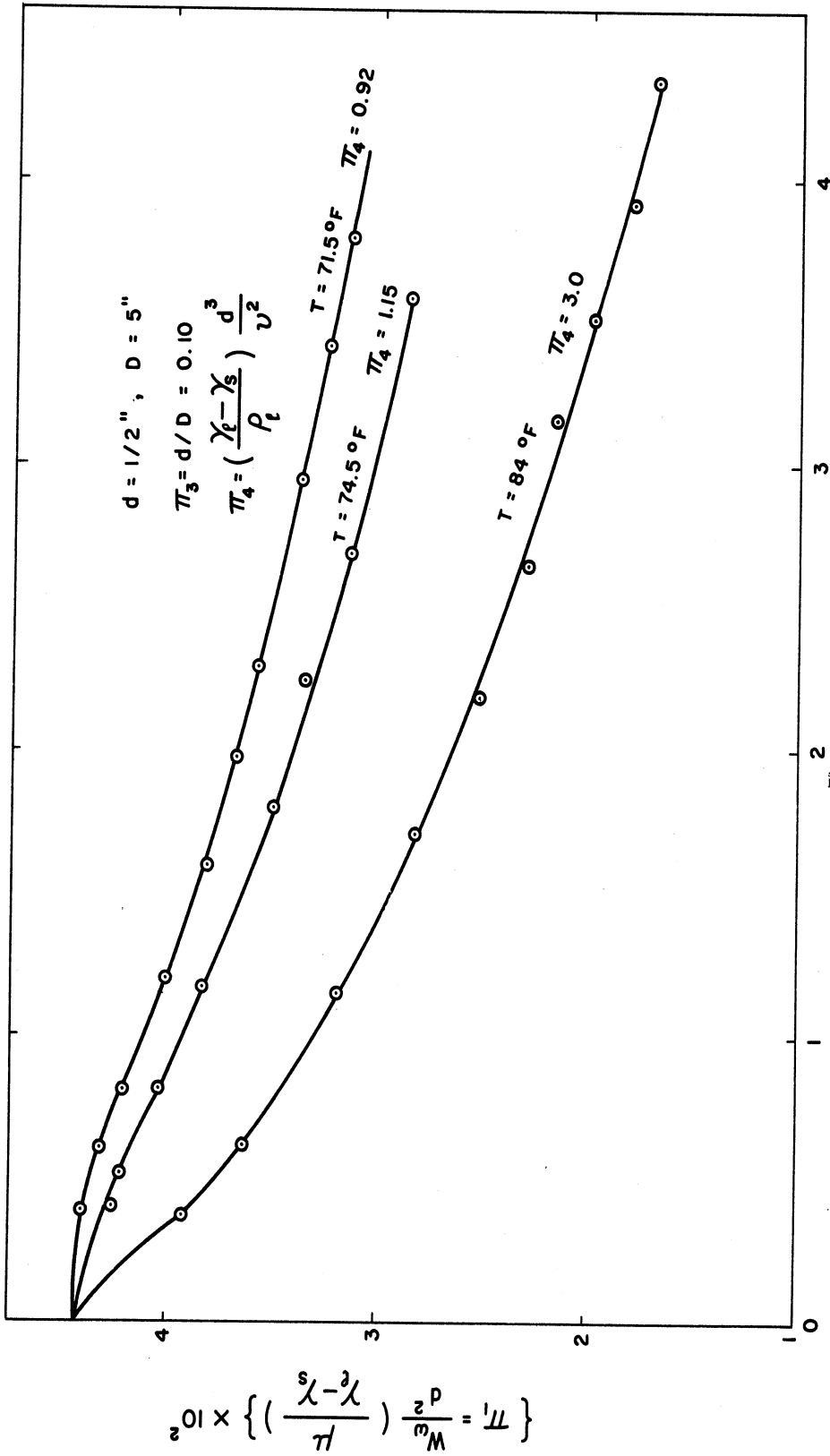
Figure 8. Curves of Constant π_4 for $\pi_3 = 0.10$.
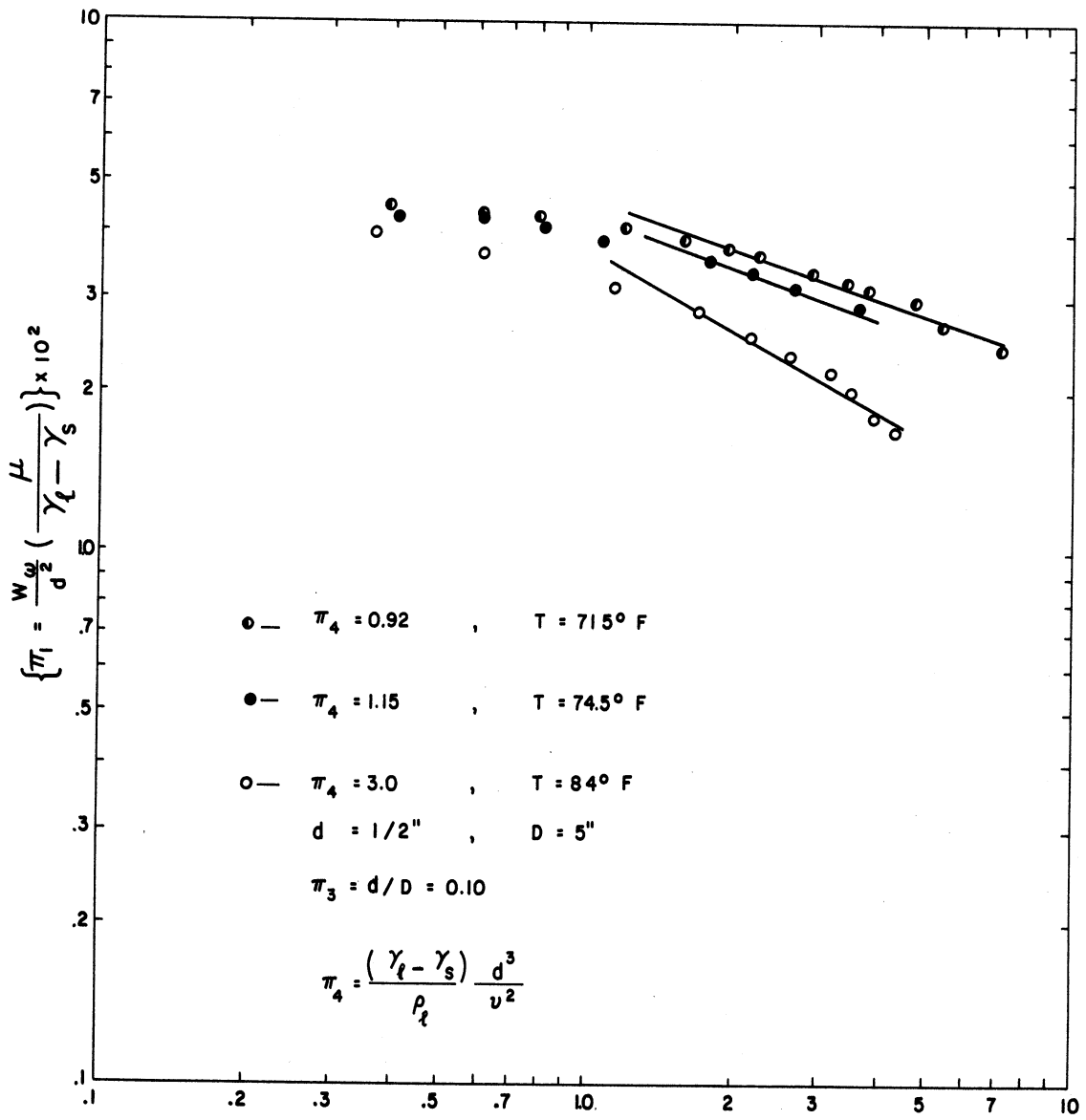
Figure 8(a). Curves of Constant π_4 for $\pi_3 = 0.10$.
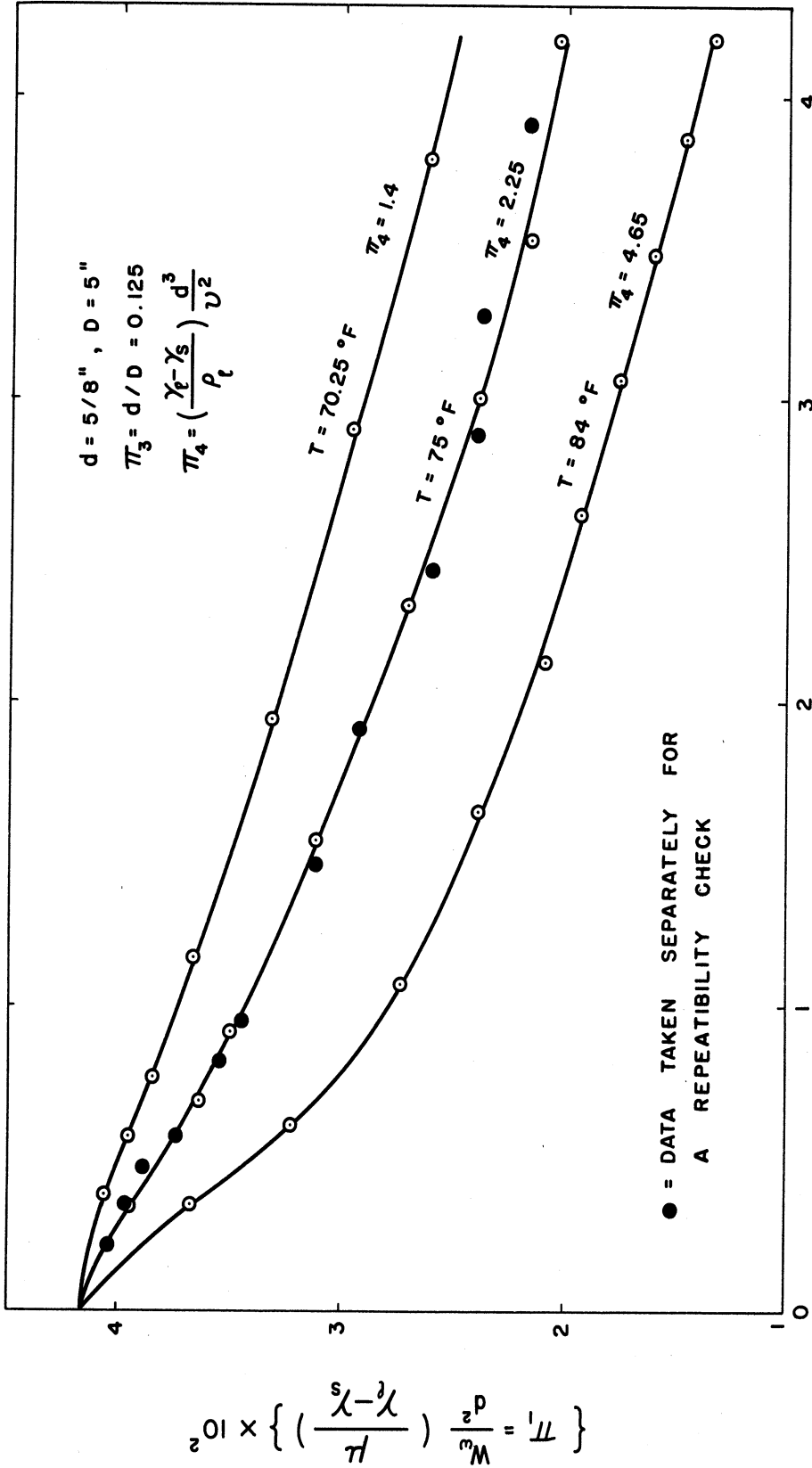
Figure 9. Curves of Constant π_4 for $\pi_3 = 0.125$.
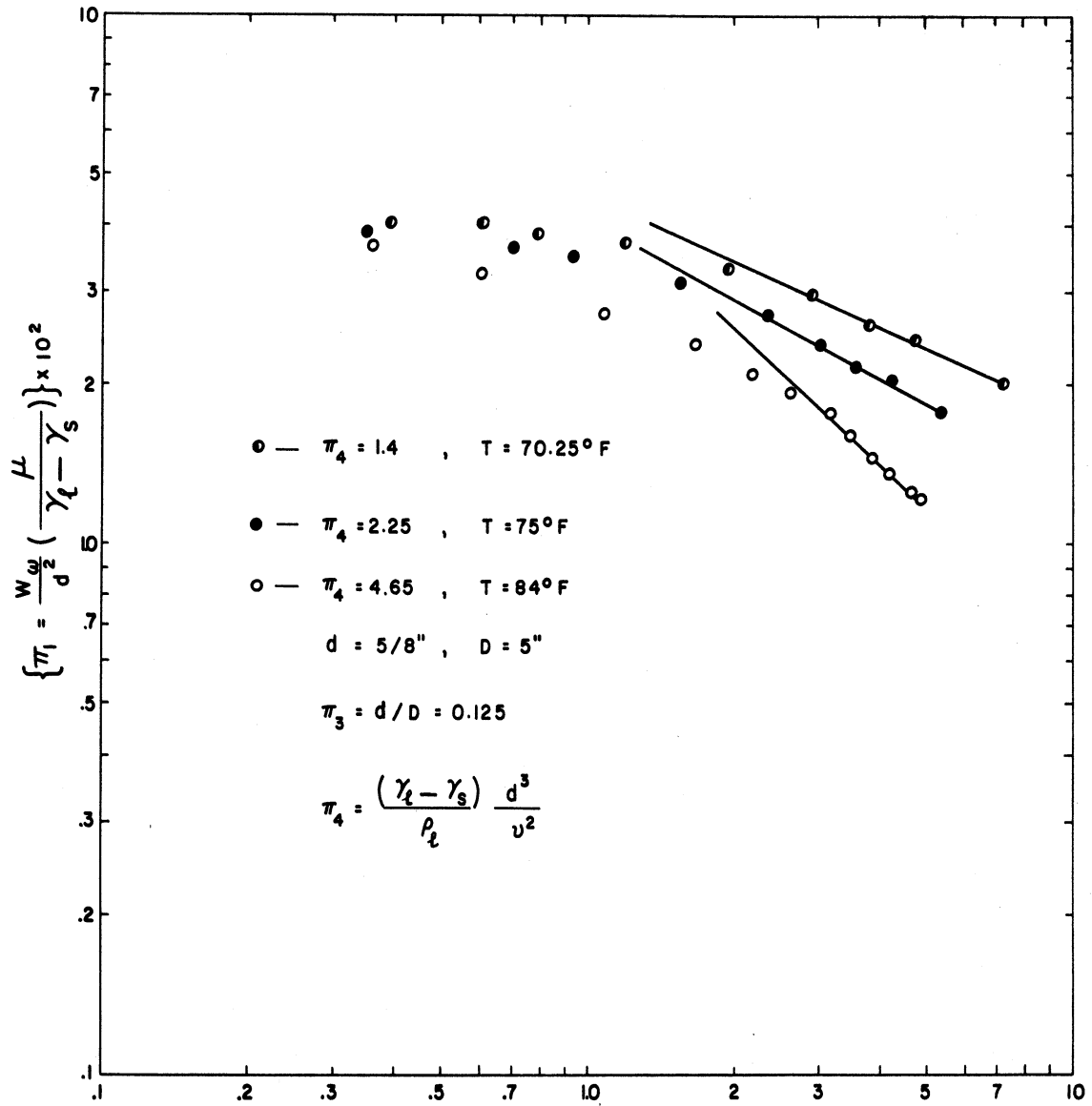
Figure 9(a). Curves of Constant π_4 for $\pi_3 = 0.125$.
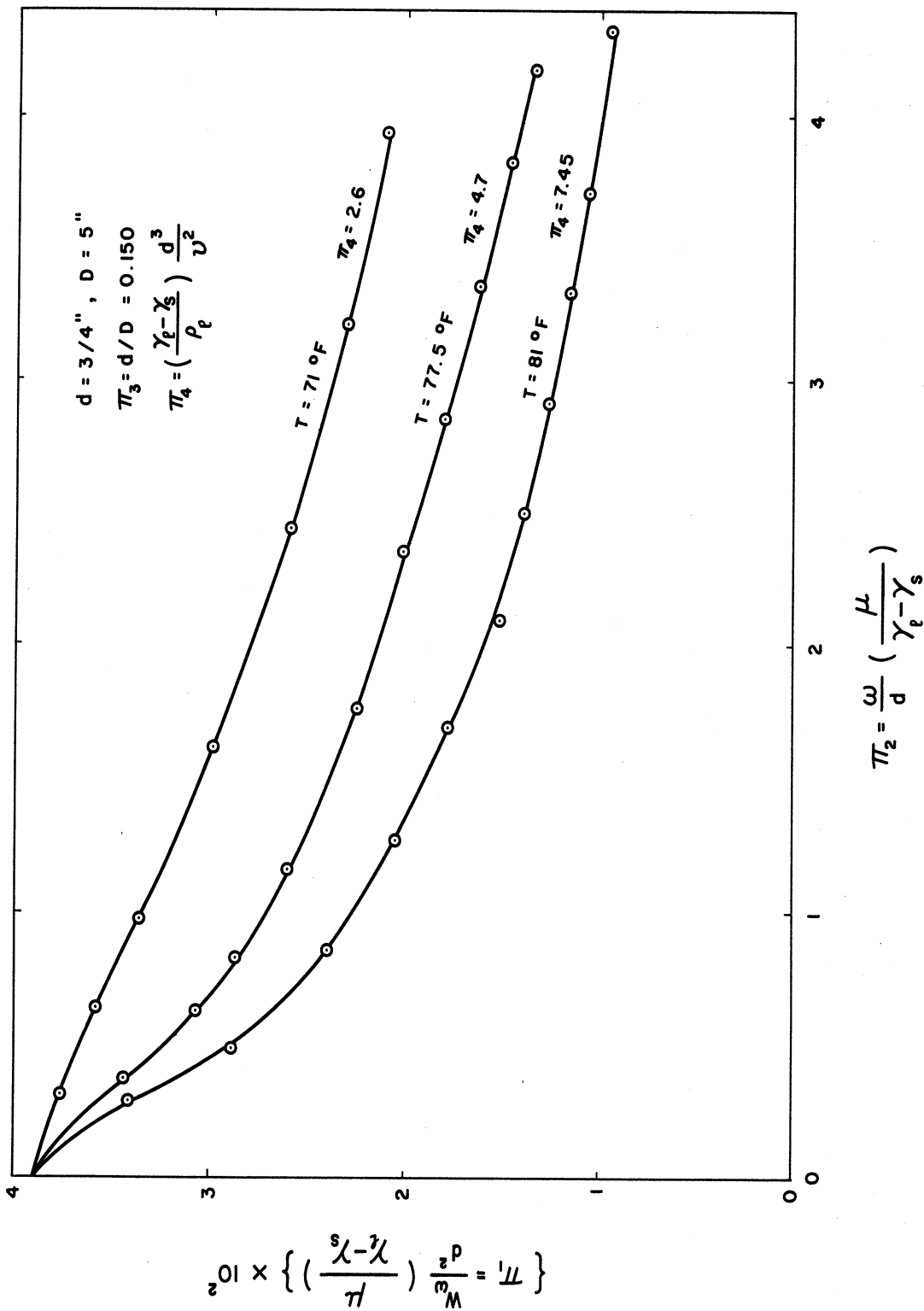
Figure 10. Curves of Constant π_4 for $\pi_3 = 0.150$.
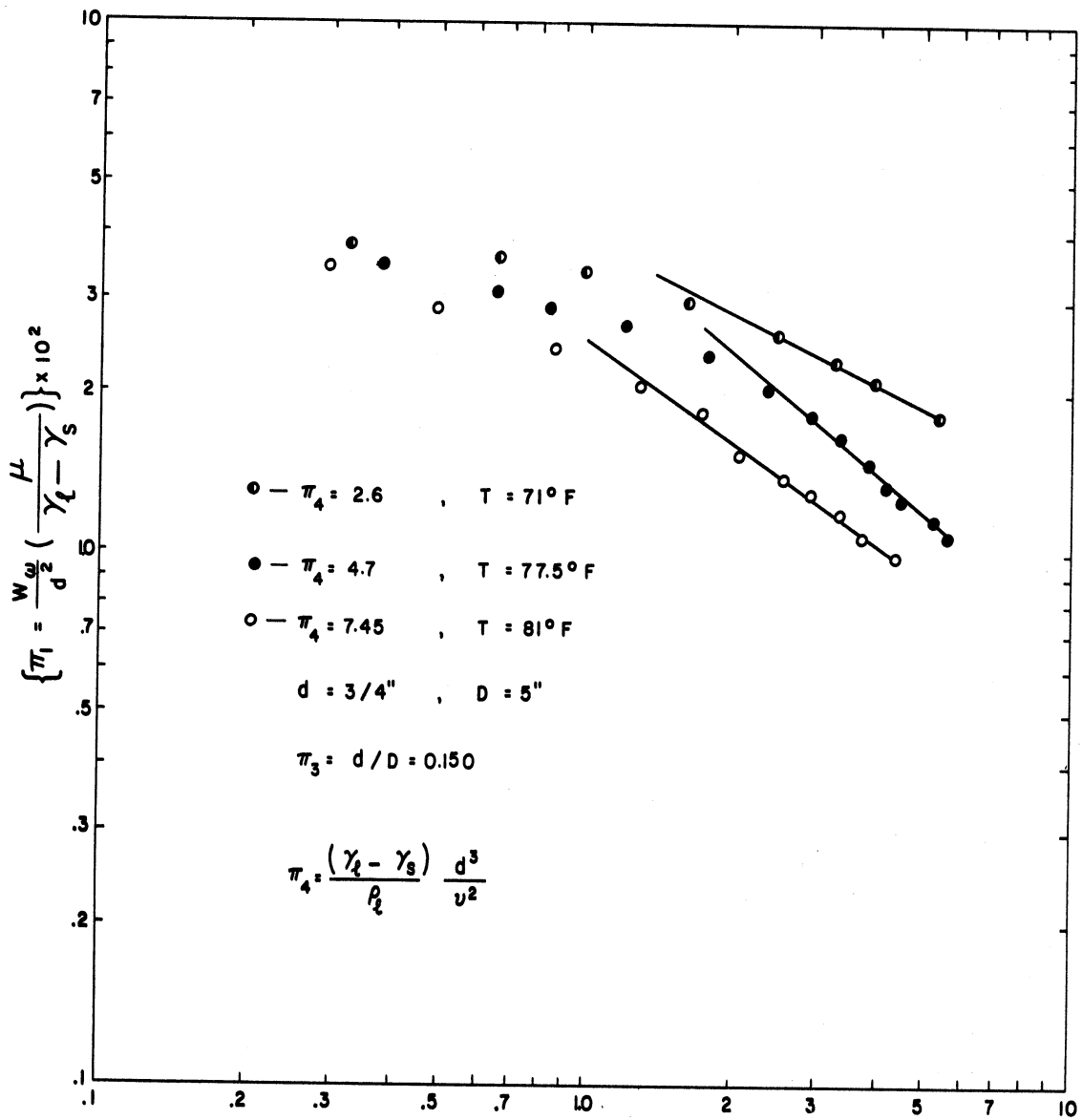
Figure 10(a). Curves of Constant π_4 for $\pi_3 = 0.150$.

Figure 11. Curves of Constant π_4 for π_3 = 0.175.
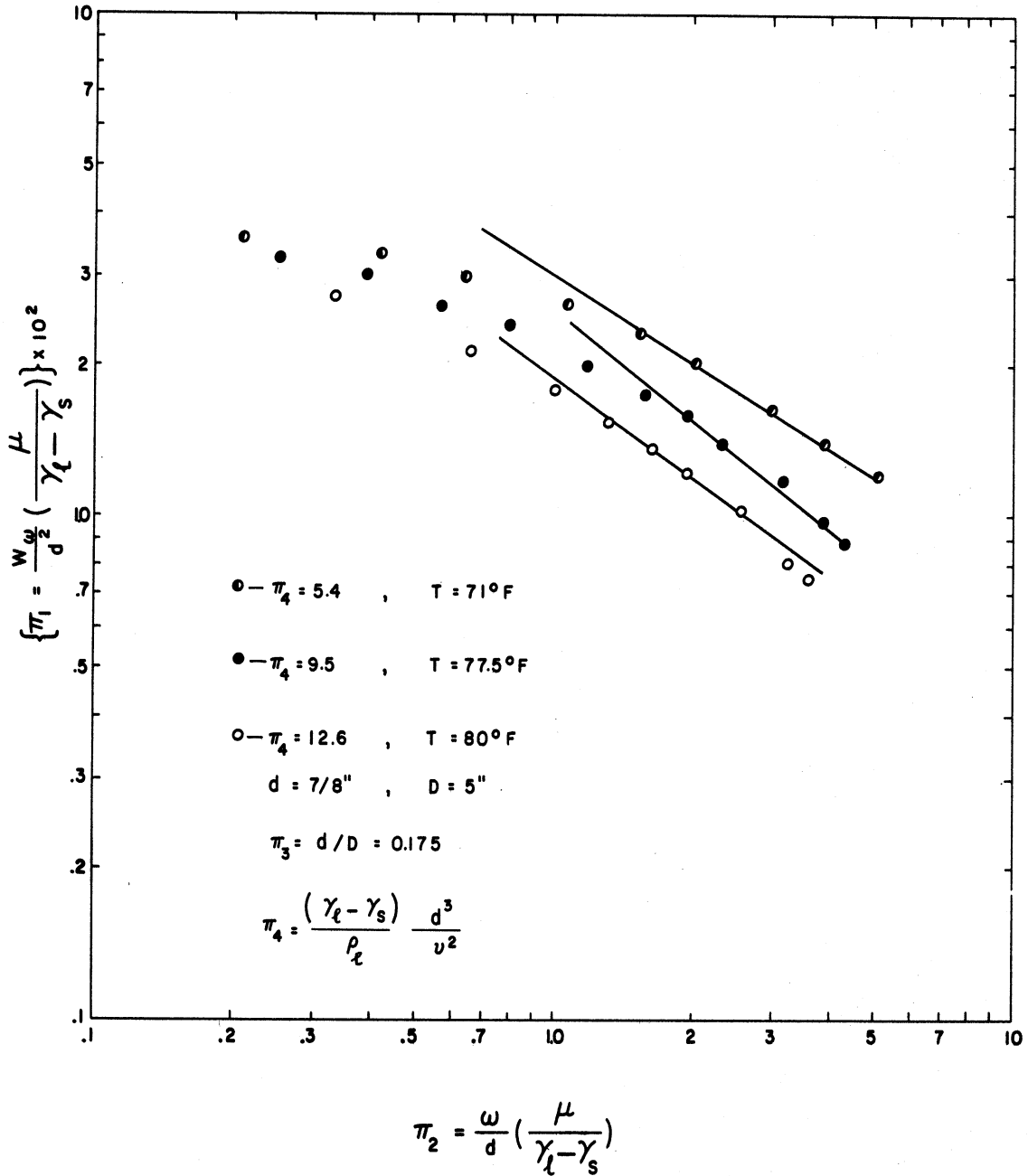
Figure 11(a). Curves of Constant π_4 for $\pi_3 = 0.175$.
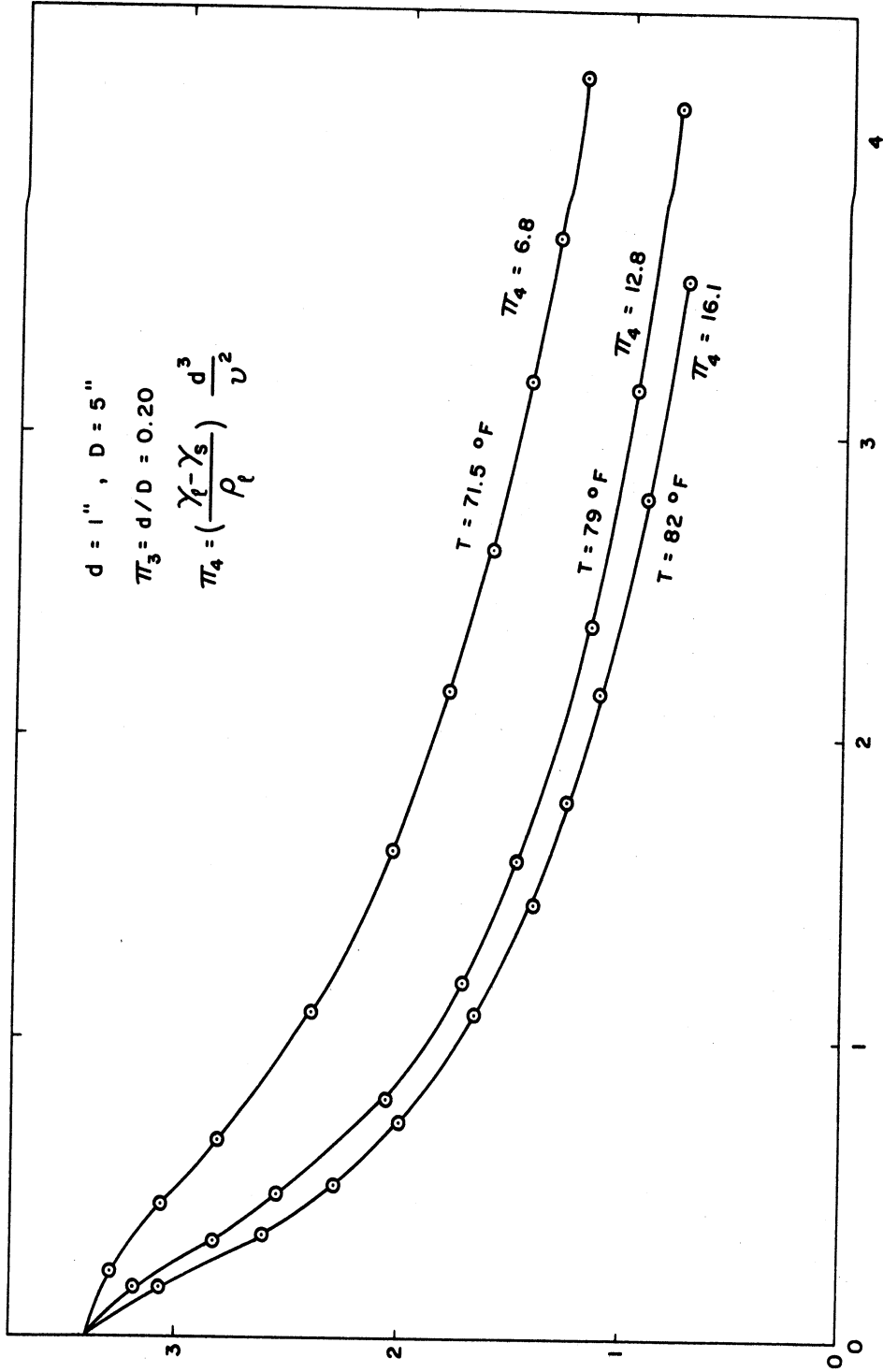
Figure 12. Curves of Constant π_4 for $\pi_3 = 0.20$.
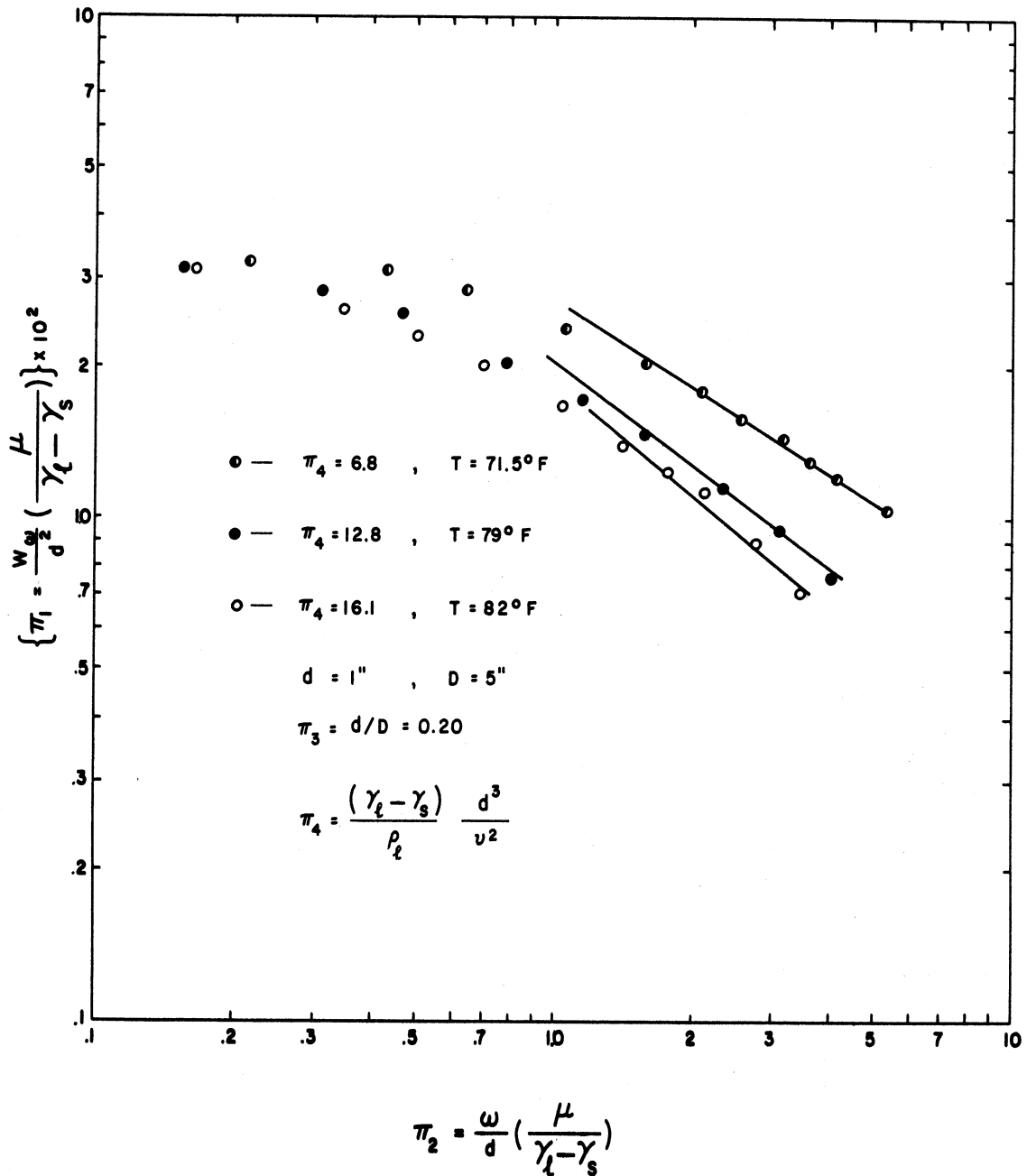
Figure 12(a). Curves of Constant π_4 for $\pi_3 = 0.20$.

$$\pi_3 = d/D = 0.225$$

$$\pi_4 = \left(\frac{\gamma_\ell - \gamma_s}{\rho_\ell}\right) \frac{d^3}{\nu^2}$$

d = 1 1/8", D = 5"

$\pi_4 = 9$

$\pi_4 = 16$

$\pi_4 = 21.5$

T = 71.5 °F

T = 78 °F

T = 81 °F

$$\pi_2 = \frac{\omega}{d}\left(\frac{\mu}{\gamma_\ell - \gamma_s}\right)$$

$$\left\{\pi_1 = \frac{W}{d^2} \frac{m}{\mu}\left(\frac{\mu}{\gamma_\ell - \gamma_s}\right)\right\} \times 10^2$$
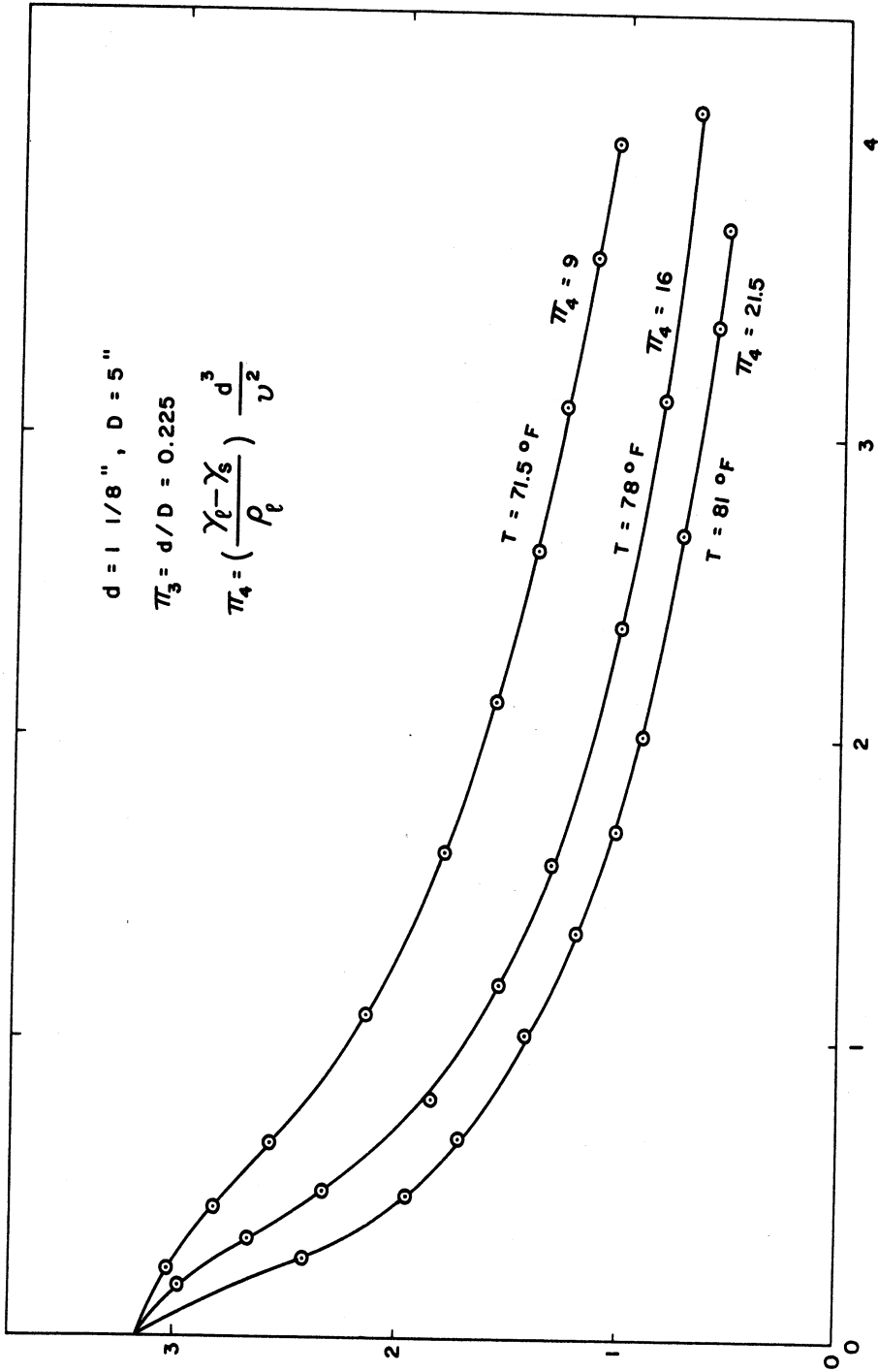
Figure 13. Curves of Constant π_4 for $\pi_3 = 0.225$.

$\left\{ \pi_1 = \dfrac{w}{d^2}\dfrac{\omega}{}\left(\dfrac{\mu}{\gamma_\ell - \gamma_s}\right)\right\}\times 10^2$

$\mathbf{0} - \pi_4 = 9$, $T = 71.5\,^\circ F$

$\bullet - \pi_4 = 16$, $T = 78\,^\circ F$

$O - \pi_4 = 21.5$, $T = 81\,^\circ F$

$d = 1/8"$, $D = 5"$

$\pi_3 = d/D = 0.225$

$\pi_4 = \dfrac{\left(\gamma_\ell - \gamma_s\right)}{\rho_\ell}\dfrac{d^3}{v^2}$

$$\pi_2 = \frac{\omega}{d}\left(\frac{\mu}{\gamma_\ell - \gamma_s}\right)$$

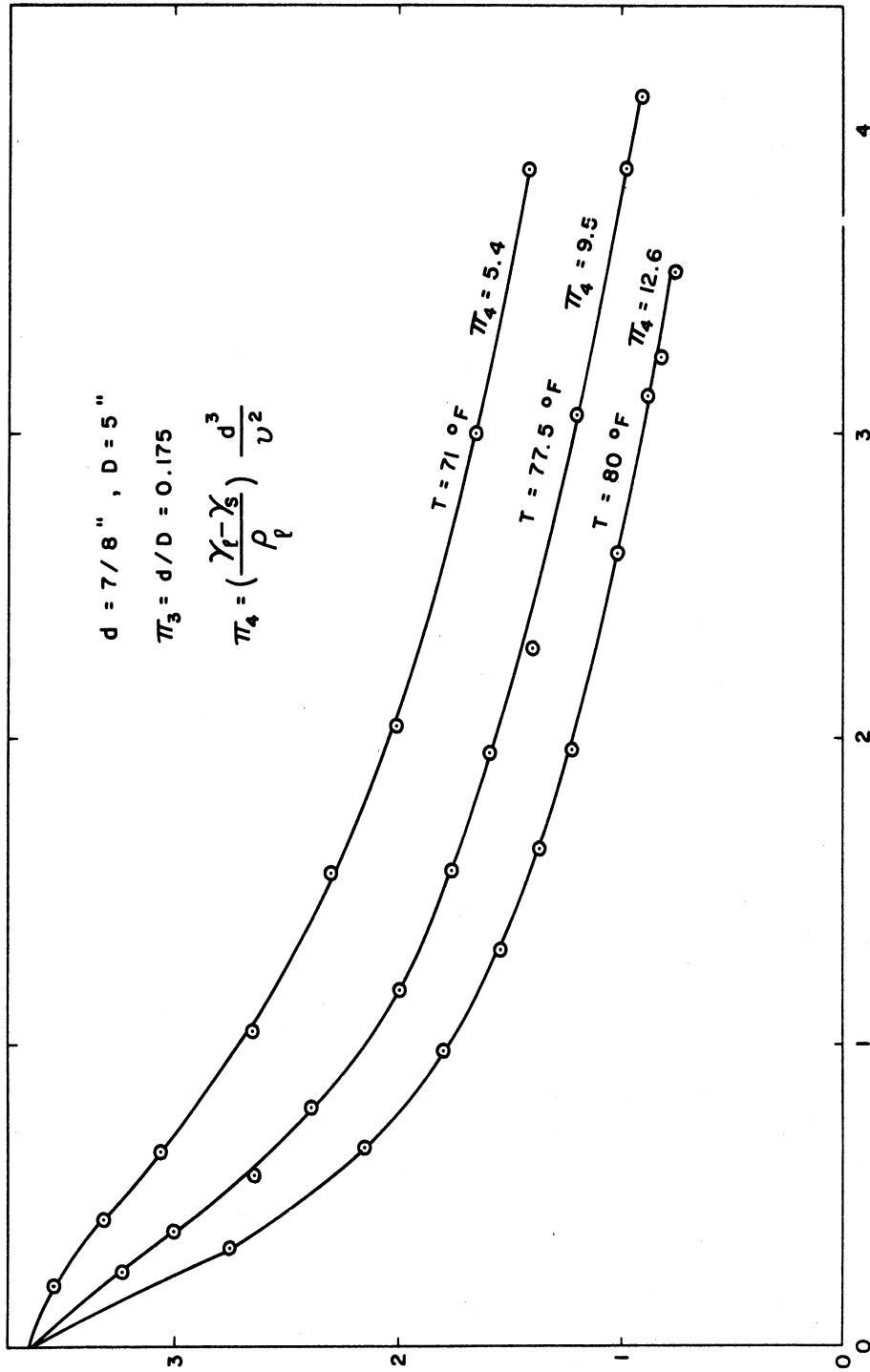Figure 13(a). Curves of Constant π_4 for $\pi_3 = 0.225$.

π_4/d^3 was held approximately constant, as stated earlier. The value of π_4 for each separate run shown in Figure 14 may be found on the corresponding curve in Figures 6 through 13 which represent the same data.

W_ω was determined by measuring the time for the sphere to travel one half foot along the axis of rotation. This was done for two adjacent test sections in order to verify that the sphere was not accele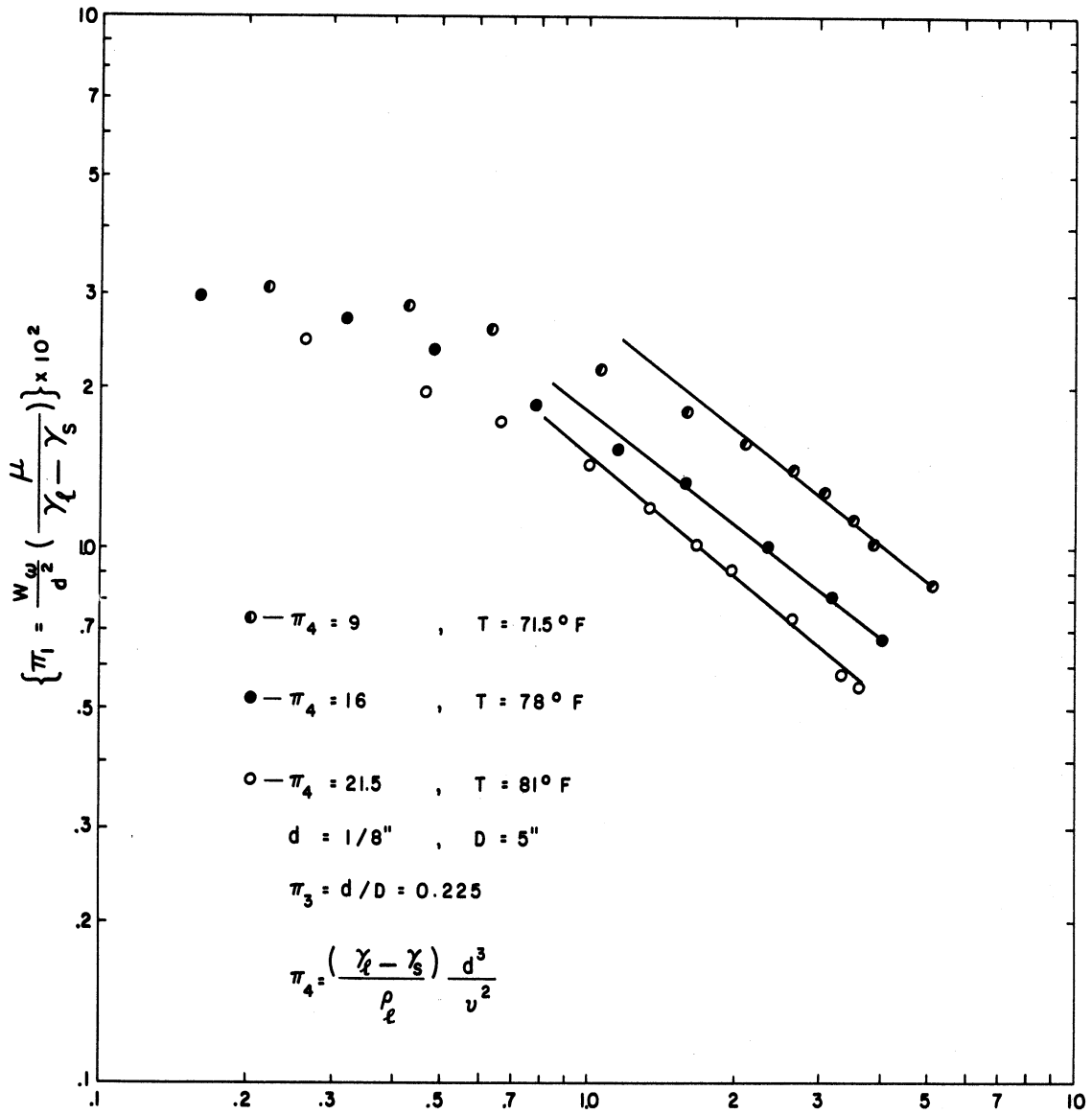rating and also as an experimental check. For the seven spheres ranging in size from 3/8 to 9/8 inch diameter, the difference in measured time for the two adjacent test sections was less than 2.5% of the total time for all tests. For the 1/4 inch diameter sphere this difference was less than 8.5%.

There are three curves for each sphere for a total of twenty four runs represented in Figures 6 through 13. In thirteen of these runs the viscosity (based on W_0) decrease from beginning of the run to the end was less than 5%, less than 10% in eight of the runs and less than 15% in three of the runs. This change in viscosity was due to small amounts of heat created by the shear stresses during the periods of starting and stopping the rotation of the fluid. An average viscosity was used for each run to calculate π_4. π_4 was also calculated by use of the data in the Appendix (Figure 18) and the mean measured temperature for the run. For twenty two runs, the difference was less than 5% and less than 7.5% for the two additional runs.

The maximum Reynolds number based on W_0, was less than 0.1 for the 3/8 and 1/4 inch diameter spheres and less than 0.7 for all the larger spheres.
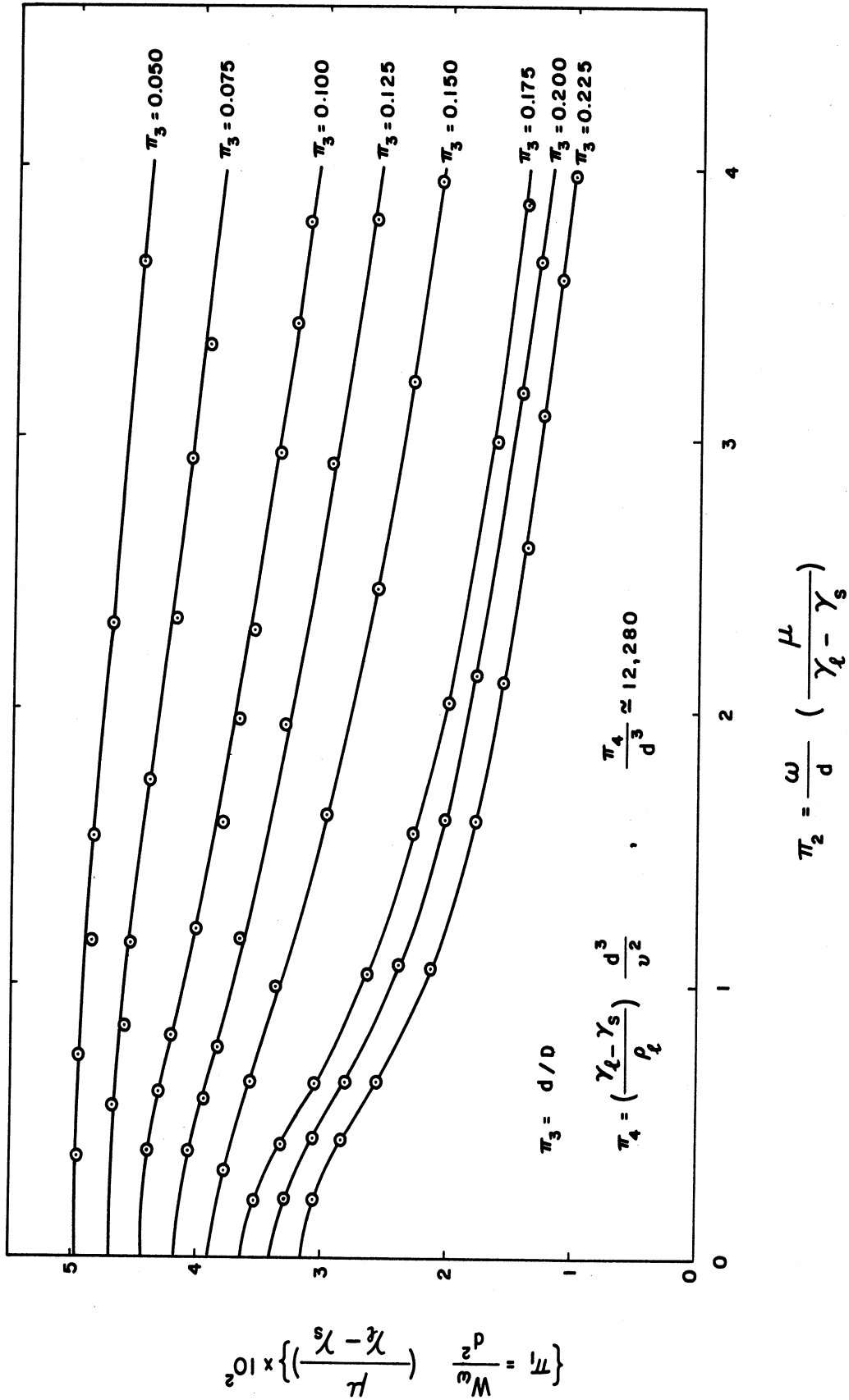
Figure 14. Curves of Constant π_3 for $\pi_4/d^3 \cong 12,280$.

$\pi_3 = d/D$

$\pi_4 = \left(\dfrac{\gamma_\ell - \gamma_s}{\rho_\ell}\right)\dfrac{d^3}{\nu^2}$, $\dfrac{\pi_4}{d^3} \cong 12,280$

$\pi_2 = \dfrac{\omega}{d}\left(\dfrac{\mu}{\gamma_\ell - \gamma_s}\right)$

$\left\{\pi_1 = \dfrac{W_\omega}{d^2}\left(\dfrac{\mu}{\gamma_\ell - \gamma_s}\right)\right\} \times 10^2$

$\pi_3 = 0.050$
$\pi_3 = 0.075$
$\pi_3 = 0.100$
$\pi_3 = 0.125$
$\pi_3 = 0.150$
$\pi_3 = 0.175$
$\pi_3 = 0.200$
$\pi_3 = 0.225$

The run for $d=5/8$ inch and $T=75°F$ was chosen at random for a repeatability check. The data acquired from both runs lie on the same curve as shown in Figure 9.

B. Motion Out from the Axis

Figure 15 is a plot in the form suggested in Figure 4 of π_1^* versus π_2^* for four values of π_3^* with π_4^*/d^3 and π_5^* held approximately constant. The diameters of the four spheres are 1/2, 3/8, 1/4 and 3/16 inch.

Figure 16 represents the data for two spheres with the same diameter (3/8 inch) but with different densities. The lighter sphere is nylon (S.G. = 1.14) and the heavier one is a hollow metal sphere with a specific gravity of 2.84. In this case π_3^* and $\pi_4^*/\gamma_s - \gamma_\ell$ is constant for two different values of π_5^*.

Figure 17 shows the data in Figure 15 and 16 plotted to a log-log scale.
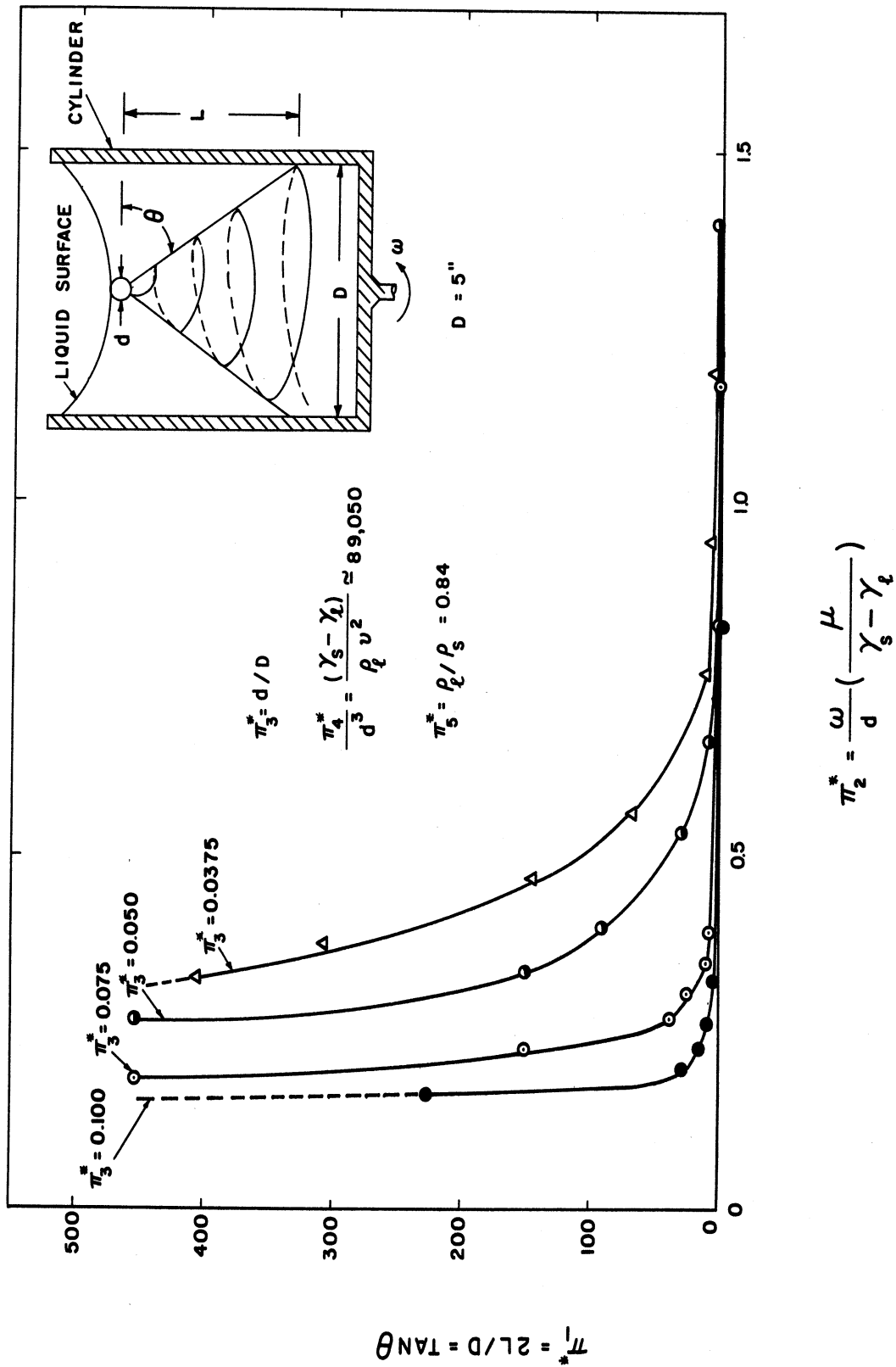
Figure 15. Curves of Constant π_3^* for $\pi_4^*/d3 \simeq 89,050$ and $\pi_5^* = 0.84$.
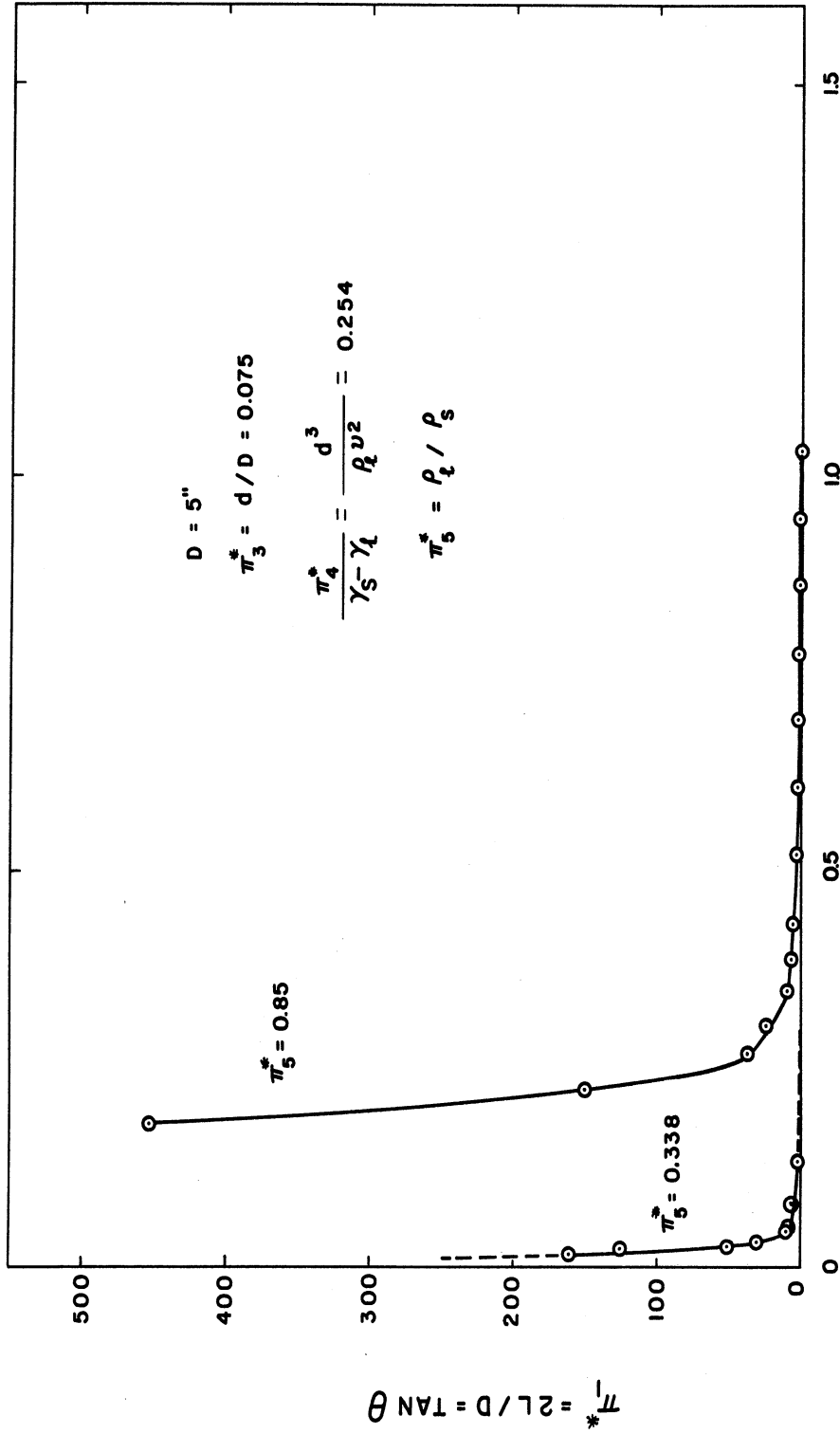
Figure 16. Curves of Constant π_5^* for $\pi_3^* = 0.075$ and $\dfrac{\pi_4^*}{\gamma_s - \gamma_\ell} = 0.254$.
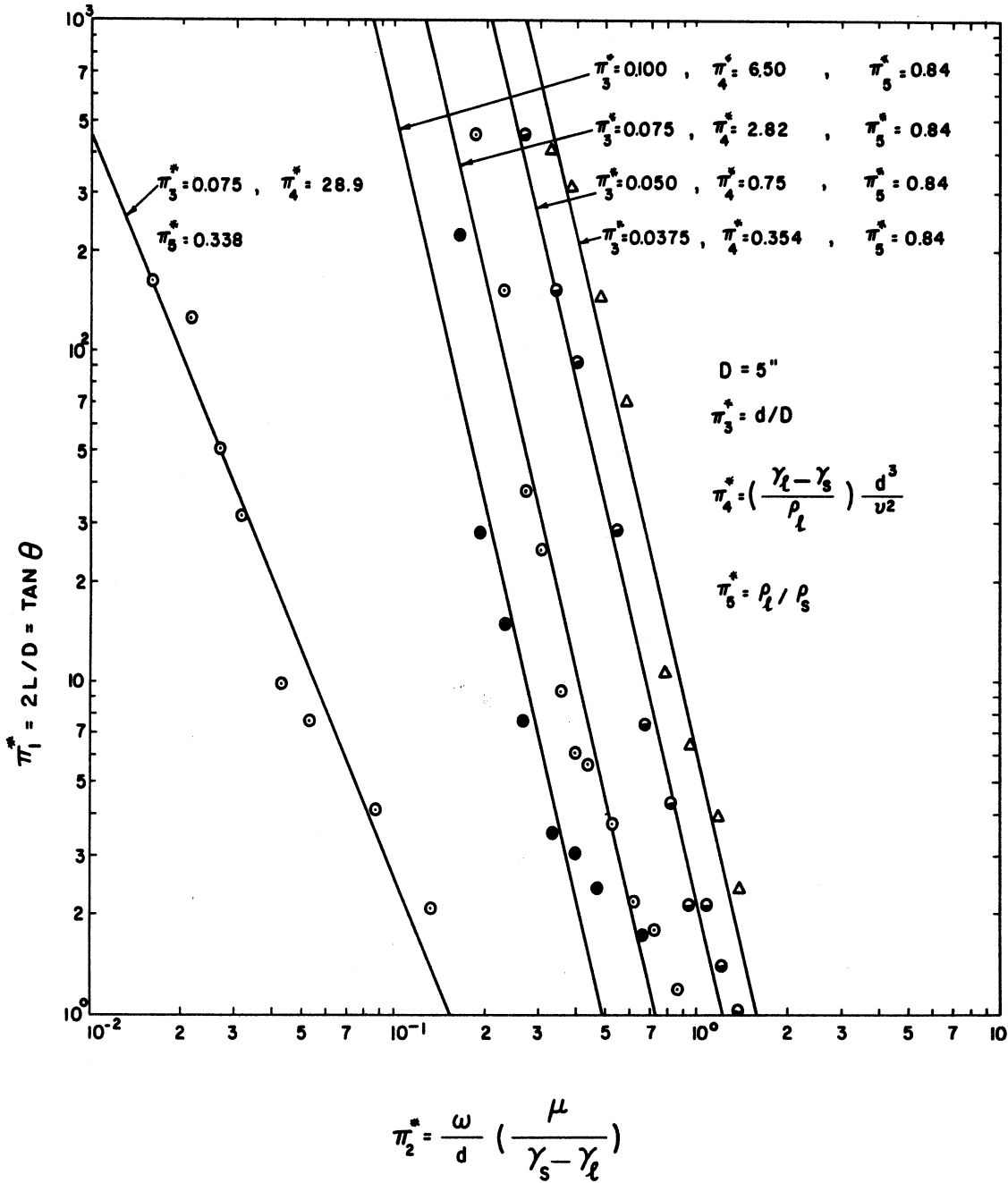
Figure 17. Curves of Constant π_3^*, π_4^*, and π_5^*.

VI. DISCUSSION OF RESULTS

A. Motion Along the Axis

The plots of the data shown in Figures 6 through 14 verify Equation (20) which was derived by dimensional analysis. The log-log plots shown in Figures 6(a) through 13(a) suggests that for higher values of π_2 the data is of the form

$$\pi_1 = C(\pi_2)^n \tag{31}$$

where C an n depend upon π_3 and π_4 .

For the special case of a cylinder with infinite radius, Equation (20) holds if $\pi_3 = d/D$ is deleted. To discuss this special case, we look at Figure 6 which represents the data with the smallest amount of wall effect assuming that the wall effect is a function of geometry only $(\frac{W_0}{W_\infty} = 0.895$ here for Stokes Flow). The velocity is only slightly decreased by rotation for $\omega < 1$. This is as expected since the Coriolis acceleration is very small and the problem is little different from the Stokes problem. Taylor[13] found that a sphere traveling slowly along the axis of a rotating inviscid fluid will push a cylindrical column of fluid along in front and behind it of the same diameter as the sphere. The data here show that the velocity decreases from the Stokes velocity, as ω is increased, more rapidly as the rotating liquid becomes less viscous. This suggests that as the viscosity of the liquid is decreased the amount of liquid affected or moved along with the sphere is increased with the limiting case being a cylindrical column as first found by Taylor. The writer

-43-

performed an experiment with a slowly moving sphere $(W_\omega \approx 0.04$ ft/sec.,

$\omega \approx 150$ rpm.) in rotating water and, with the use of potassium perman-

ganate as a dye, observed the column of fluid that the sphere pushed

along. The Reynolds number for this experiment was approximately 300.

A similar experiment with castor oil is difficult. The writer, however,

by injecting a mixture of castor oil and linseed oil, which had been

dyed black, along the axis of rotation, did observe that some fluid near

the sphere was pushed along with the sphere but the results were incon-

clusive as to the amount and shape of this fluid.

B. Motion Out from the Axis

The data represented in Figure 15 indicates that as π_2^* decreases

beyond a certain value θ is almost 90 degrees. Let the value of the

angular velocity associated with the π_2^* at which the angle θ appears

to approach 90 degrees represent a critical value of angular rotation

(ω_{c1}) below which the motion of a given sphere in a given liquid will

for all practical purposes remain stable along the axis of rotation. The

data here indicates that ω_{c1} increases as the sphere size increases.

The method of taking data for this experiment becomes inherently

less accurate as π_1^* approaches zero. Very little data were obtained for

$\pi_1^* < 1$. Also, the values of $L > 28$ inches were found by extrapolation.

Let the angular velocity at which the angle θ approaches 45

degrees $(L=2.5$ inches) be arbitrarily defined as the upper critical value

(ω_{c2}). The four runs shown in Figure 15 represents data for four sizes

of nylon spheres in castor oil. The average temperature, density and viscosity for the four runs is 74°F, 1.86 slugs/ft^3 and 0.01544 lb sec/ft^2. The approximate values of ω_{c1} and ω_{c2} in rad/sec are

$$
\left.\begin{array}{l}
\omega_{c1} \approx 3 \\
\omega_{c2} \approx 13
\end{array}\right\} \qquad \text{for d = 3/16 inch,}
$$

$$
\left.\begin{array}{l}
\omega_{c1} \approx 3.75 \\
\omega_{c2} \approx 20
\end{array}\right\} \qquad \text{for d = 1/4 inch,}
$$

$$
\left.\begin{array}{l}
\omega_{c1} \approx 3.85 \\
\omega_{c2} \approx 23
\end{array}\right\} \qquad \text{for d = 3/8 inch,} \qquad\qquad (32)
$$

and

$$
\left.\begin{array}{l}
\omega_{c1} \approx 4.2 \\
\omega_{c2} \approx 24
\end{array}\right\} \qquad \text{for d = 1/2 inch.}
$$

The data plotted in Figure 16 are for two 3/8-inch diameter spheres of different density. One was a hollow metal sphere (S.G. = 2.84) and the other was nylon (S.G. = 1.14). The effect of increasing the density of a sphere while keeping its size constant is to decrease ω_{c1} and increase ω_{c2}. The approximate values of ω_{c1} and ω_{c2} for the metal sphere are

$$
\left.\begin{array}{l}
\omega_{c1} \approx 1.2 \\
\omega_{c2} \approx 34
\end{array}\right\} \qquad \text{for d = 3/8 inch,} \qquad (33)
$$

and the values for the nylon sphere are given in (35).

The log-log plots in Figure 17 of all the data taken suggests that the data is of the form

$$\pi_1^* = A \, (\pi_2^*)^n ,$$

<div align="right">(34)</div>

where n depends on π_5^* ($n = 3.898$ for the nylon spheres and $n = 2.224$ for the hollow metal sphere) and A depends on π_3^* and π_4^*.

VII. CONCLUSIONS

The following conclusions can be drawn for motion along the axis:

1) If the sphere is less dense than the liquid and is re-leased on the axis of rotation, the free motion will remain along the axis of rotation.

2) The sphere rotates at very much the same angular velocity as the cylinder.

3) The velocity of the sphere in a liquid with constant temperature decreases from the Stokes velocity as the angular rotation is increased. Specific results are given in Figures 6 through 14.

4) The rate of decrease of velocity, as the angular rota-tion is increased, increases as the viscosity of the liquid medium is decreased. Thus, the effect of viscosity is to decrease the amount of fluid affected or moved along with the sphere.

5) From the equations of motion, it is concluded that it is the effect of the Coriolis acceleration that leads to a terminal velocity less than the Stokes velocity for the sphere provided that the assumed slow motion is valid.

6) The velocity of the sphere along the axis is given by

$$W_\omega = \frac{d^2(\gamma\ell - \gamma s)}{\mu} \, f[\frac{\omega}{d}(\frac{\mu}{\gamma\ell - \gamma s}), \, \frac{d}{D}, (\frac{\gamma\ell - \gamma s}{\rho\ell}) \, \frac{d^3}{\nu^2}] \, . \qquad (20)$$

The function is given graphically in Figures 6 through 14.

The following conclusions can be drawn for the motion out from the axis:

1) There exists a critical value of angular rotation (ω_{c1}) below which the motion of a given sphere in a given liquid will remain stable, for the length of the column used at least, along the axis of rotation. The data indicate that the value of ω_{c1} increases as the sphere size is increased.

2) The value of angular velocity (ω_{c2}) at which the angle Θ approaches the arbitrarily chosen value of $\pi/4$ increases as the size of sphere is increased.

3) The effect of increasing the density of a sphere while keeping its size constant is to decrease ω_{c1} and increase ω_{c2}.

4) The angle Θ is given by

$$\text{Tan } \Theta = f[\frac{\omega}{d}(\frac{\mu}{\gamma s - \gamma \ell}), \frac{d}{D}, (\frac{\gamma s - \gamma \ell}{\rho \ell}) \frac{d^3}{v^2}, \frac{\rho s}{\rho \ell}] . \qquad (24)$$

The data herein suggests that Equation (24) is of the form

$$\text{Tan } \Theta = F(\frac{d}{D}, \frac{\gamma s - \gamma \ell}{\rho \ell} \frac{d^3}{v^2}) [\frac{\omega}{d}(\frac{\mu}{\gamma s - \gamma \ell})]^{G(\frac{\rho s}{\rho \ell})} . \qquad (34)$$

Specific results are given in Figures 15, 16, and 17.

VIII. SUGGESTIONS FOR FUTURE WORK

Future work should be devoted to obtaining a solution to the differential system for motion along the axis; first, for the special case of an infinite fluid and secondly, for the case of a finite cylinder. Once the solution for an infinite medium is accomplished, an experimental wall effect can be obtained by use of the experimental data herein. The experimental results in this thesis can also be used to guide the theoretical solution for the case of a finite cylinder. Once this is accomplished, a theoretical wall effect can be derived and compared to the experimental wall effect.

The experimental work should next be carried out for a sphere at intermediate and high Reynolds numbers. Then, the experiments could include other shapes of bodies of revolution, such as the ellipsoid and cylinder, for all three ranges of Reynolds numbers.

It would also be interesting to extend the experiments of motion out from the axis to higher Reynolds numbers and to other shapes.

APPENDIX

TABLE OF EQUATIONS OF THE PHYSICAL PROPERTIES OF
CASTOR OIL AS A FUNCTION OF TEMPERATURE

The coefficient of expansion of castor oil in terms of density
is 0.00066.

$$\rho = 0.9849 - 3.667 \quad 10^{-4} T \quad gm/cm^3 \; ,$$

$$\rho = 1.9107 - 7.113 \quad 10^{-4} T \quad slug/ft^3 ,$$

$$\gamma = 61.4873 - 2.2891 \quad 10^{-2} T \quad lb/ft^3 \; ,$$
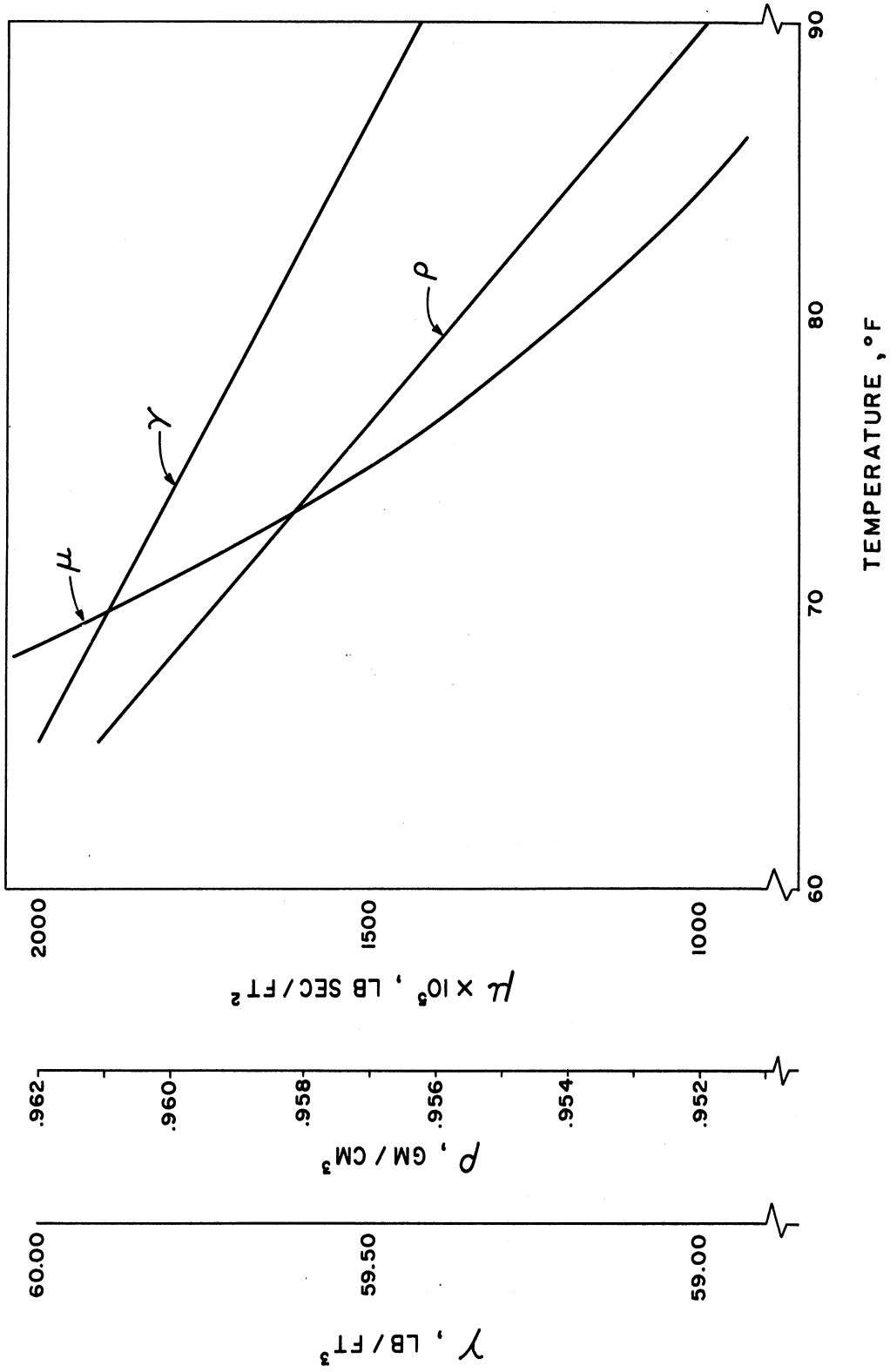
where $T = °F.$

Figure 18. Plot of the Physical Properties of Castor Oil Versus Temperature.

BIBLIOGRAPHY

1. Fidleris, V. and Whitmore, R. L. "Experimental Determination of the Wall Effect for Spheres Falling Axially in Cylindrical Vessels." Brit. J. Appl. Phys., 12, (1961), 490-4.

2. Grace, S. F. "Free Motion of a Sphere in a Rotating Liquid Parallel to the Axis of Rotation." Roy. Soc. Proc., A102, (1922), 89-110.

3. Grace, S. F. "Free Motion of a Sphere in a Rotating Liquid at Right Angles to the Axis." Roy. Soc. Proc., A104, (1923), 278-301.

4. Grace, S. F. "A Spherical Source in a Rotating Liquid." Roy. Soc. Proc., A105, (1924), 532-43.

5. Grace, S. F. "On the Motion of a Sphere in a Rotating Liquid." Roy. Soc. Proc., A113, (1926), 46-77.

6. Lamb, H. Hydrodynamics. New York: Dover Publications, 6th Ed., (1932), Chapt. XII.

7. Squire, H. B. "Rotating Fluids." Surveys in Mechanics, (1956), 139-161.

8. Taylor, G. I. "Motion of Solids in Fluids when the Flow is not Irrotational." Roy. Soc. Proc., A93, (1917), 99-113.

9. Taylor, G. I. "Experiments with Rotating Fluids." Camb. Phil. Soc. Proc., 20, (1921), 326-29.

10. Taylor, G. I. "Experiments with Rotating Fluids." Roy. Soc. Proc., A100, (1922), 114-21.

11. Taylor, G. I. "The Motion of a Sphere in a Rotating Liquid." Roy. Soc. Proc., A102, (1922), 180-9.

12. Taylor, G. I. "Experiment on the Motion of Solid Bodies in Rotating Fluids." Roy. Soc. Proc., A104, (1923), 213-18.

13. Taylor, G. I. "Experiments with Rotating Fluids." Proc. 1st. Int. Congr. Appl. Mech., (1924), 89-96.

14. Proudman, J. "On the Motion of Solids in a Liquid Possessing Vorticity." Roy. Soc. Proc., A92, (1916), 408-24.